

Medical University of South Carolina

MEDICA

MUSC Theses and Dissertations

2010

Proteomic Analysis Of Plasma Exosomes Reveals That Kappa:Lambda Ratio Predicts Severe Acute Graft-Versus-Host Disease

Joseph Alge

Medical University of South Carolina

Follow this and additional works at: <https://medica-musc.researchcommons.org/theses>

Recommended Citation

Alge, Joseph, "Proteomic Analysis Of Plasma Exosomes Reveals That Kappa:Lambda Ratio Predicts Severe Acute Graft-Versus-Host Disease" (2010). *MUSC Theses and Dissertations*. 22.

<https://medica-musc.researchcommons.org/theses/22>

This Thesis is brought to you for free and open access by MEDICA. It has been accepted for inclusion in MUSC Theses and Dissertations by an authorized administrator of MEDICA. For more information, please contact medica@musc.edu.

Proteomic Analysis of Plasma Exosomes Reveals That Kappa:Lambda Ratio
Predicts Severe Acute Graft-Versus-Host Disease

By


Joseph Alge


A dissertation submitted to the faculty of the Medical University of South Carolina
in partial fulfillment of the requirements for the degree of Master's in Clinical
Research in the College of Graduate Studies.

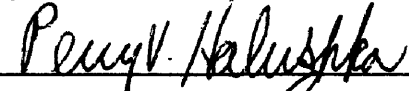
2010

Approved by:

Chairman, Advisory Committee







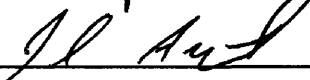


Table of Contents

Abstract.....	iii
Chapters	
1 Introduction.....	1
2 Review of the Literature.....	2
Allogeneic Hematopoietic Stem Cell Transplantation and Graft-Versus-Host Disease.....	2
Historical Significance of Exosomes.....	6
Exosome Biogenesis.....	7
Immunobiology of Exosomes.....	10
Exosomes and Biomarker Discovery.....	21
3 Methods.....	24
Protocol Development.....	24
Reproducibility Experiment.....	28
Acute GVHD Biomarker Discovery.....	31
4 Results and Discussion.....	37
Protocol Development.....	37
Reproducibility Experiment.....	41
Acute GVHD Biomarker Discovery.....	46
5 Conclusion and Future Directions.....	58
6 Bibliography.....	60
7 Appendix: iTRAQ Data Analysis Report	

Abstract

Background: Acute Graft-Versus-Host disease (acute GVHD) is an often fatal, inflammatory multi-organ disease driven by T cell alloreactivity directed toward host tissues. One of the chief obstacles to improving outcomes of acute GVHD patients is timely diagnosis. Currently, acute GVHD is diagnosed clinically, once the symptoms are fully manifested. However, it is clear that important immunologic events occur prior to the occurrence of symptoms. A biomarker that could predict disease during the asymptomatic period could improve patient outcomes by allowing for earlier intensification of immunosuppressant therapy. Exosomes are an attractive target for acute GVHD biomarker discovery. They contain a variety of cellular components and are easily obtained from bodily fluids. Furthermore, the cell types implicated in acute GVHD pathophysiology produce exosomes with strong immunomodulatory effects.

Methods: A differential centrifugation protocol was developed to isolate exosomes from cryopreserved plasma. The presence of exosomes in the final pellet was confirmed by Western blotting of known exosome markers and by electron microscopy. This protocol was used to isolate exosome-enriched pellets from 5 ml plasma samples obtained on posttransplantation day 7 from 7 patients (N=7) who had undergone allogeneic hematopoietic stem cell transplantation. Three of these patients (cases) later developed severe acute GVHD (grade C or D), whereas 4 patients did not develop acute GVHD of any grade (controls). Proteomic analysis was performed on exosome pellets using liquid chromatography-tandem mass spectrometry and iTRAQ labeling, which allowed us to compare the relative quantities of identified proteins between cases and controls.

Results: We made 33 protein identifications. iTRAQ analysis did not demonstrate any statistically significant differences between cases and controls. Despite this limitation, our data did show trends toward differences in the relative abundances of some proteins. Specifically, there was a trend toward increased IgG3 constant region in cases (median case:control ratio= 1.36; credible interval of case:control ratio= 0.857, 2.19), increased lambda light chain constant region in cases (median case:control ratio= 1.35; credible interval of case:control ratio= 0.844, 2.07) and decreased kappa light chain constant region in cases (median case:control ratio=0.847; credible interval of case:control ratio=.0586, 1.21). Further statistical analysis to compare the kappa:lambda ratios in cases compared controls showed that the median case:control kappa:lambda ratio was 0.63, with a 95% CI of 0.377, 1.027 (p=0.011). **Conclusion:** Differences in kappa:lambda ratios, early after allogeneic hematopoietic stem cell transplantation may be predictive of the development of acute GVHD. Future studies will be directed toward validation of these results.

Introduction

Allogeneic hematopoietic stem cell transplantation (allo-HSCT) is curative for a variety of malignant and non-malignant hematologic conditions. The most important complication resulting from this procedure is acute Graft-Versus-Host disease (acute GVHD), an inflammatory, multi-organ disease driven by T-cell alloreactivity directed toward host tissues. The treatment of choice, high dose corticosteroids, is often ineffective, and acute GVHD is consequently the leading cause of non-relapse mortality in patients who have undergone allo-HSCT. One of the most significant barriers to the adequate treatment of acute GVHD is timely initiation of therapy, which is limited by current methods of diagnosis. Acute GVHD is diagnosed on clinical grounds, once the manifestations of the disease are fully established. However, it is clear that key immunologic events occur during an asymptomatic phase. Thus, a biomarker that could be used to diagnoses acute GVHD before the appearance of symptoms would be clinically useful, because it would allow for intensification of immunosuppression earlier in the course of the disease. Exosomes, membrane bound nanovesicles derived from the multivesicular body, are an attractive potential source for acute GVHD biomarker discovery, since they contain cellular components such as protein and RNA, and are released by a plethora of activated cell types implicated in acute GVHD. Moreover, they can be isolated from bodily fluids, such as plasma.

Review of the Literature

I. Allogeneic Hematopoietic Stem Cell Transplantation and Graft-Versus-Host Disease

Allogeneic hematopoietic stem cell transplantation (allo-HSCT) represents a curative therapy for many diseases, ranging from rare immunodeficiencies to hematologic cancers. More than 25,000 transplants are performed annually worldwide, and its usage is increasing.[1, 2] But allo-HSCT is not without its risks. Patients who undergo this procedure may develop graft versus host disease (GVHD). GVHD is the major cause of non-relapse mortality in these patients. It has two forms, acute and chronic, which traditionally are temporally differentiated by how soon they occur following transplantation. The former is the subject of this research project.

Acute GVHD classically occurs within the first 100 days after the transplant. It is a devastating disease in which immunocompetent T lymphocytes from the donor react with tissues of the recipient, or host. The most important determinant of a patient's risk of developing acute GVHD is the degree of histocompatibility between the donor and the recipient. Therefore, great care is taken to find a donor who is an HLA match for the recipient, that is someone who shares the same alleles for the relevant Human Leukocyte Antigen (HLA) loci.

However, even in cases of HLA identity, acute GVHD can still occur due to the presence of polymorphisms in the less well-characterized minor histocompatibility antigens.[3] Therefore, in order to further mitigate the risk of developing acute GVHD, patients undergoing allo-HSCT are given prophylactic immunosuppression with a calcineurin inhibitor and either mycophenolate mofetil or methotrexate. Despite HLA matching and prophylactic immunosuppression, approximately 40% of allogeneic HSCT recipients will develop acute GVHD requiring treatment with high dose corticosteroids, the therapy of choice.[2]

The clinical presentation of acute GVHD primarily involves three organs: the skin, the gastrointestinal tract, and the liver. Clinical manifestations include a maculopapular rash, nausea, anorexia, bloody or watery diarrhea, severe abdominal pain, and cholestatic hyperbilirubinemia.[2] The severity of acute GVHD is determined by the extent of involvement of the aforementioned organ systems, and cases are assigned a grade (A through D)[4]. Grades C and D are considered clinically severe and very severe, respectively, and they require aggressive immunosuppressive treatment. Unfortunately, treatment is often ineffective, and more than half of cases are refractory.[5] Moreover, more severe cases are less likely to respond to treatment.[6] Grades C and D acute GVHD have a 5 year survival rate of 25% and 5%, respectively.[7]

The development of acute GVHD may be understood as a multi-stage process. The first event is the priming of the immune response, triggered by tissue damaged during the pretransplant conditioning regimen.[8] It follows a massive release of proinflammatory cytokines and stimulation of antigen-

presenting-cells (APCs) of both host and donor origin.[9] The second stage is the activation of donor originated T cell, mostly by interaction with the APCs.[10] The third stage comprises the expansion of alloreactive T cells and differentiation into a Th1 or Th2 phenotype.[11] During the fourth stage, activated alloreactive T cells migrate to target tissues leading to the fifth and last stage, the tissue damage mediated by massive release of effector molecules such as FasL, TNF-alpha, TRAIL, interferon-gamma, perforin, and granzymes.[12, 13] It is the result of this tissue damage that produces the aforementioned symptoms of acute GVHD.

One of the main obstacles to the management of acute GVHD is diagnosis. Currently, it is diagnosed on clinical grounds. However, as mentioned previously, symptoms do not appear until the fifth and final stage of the disease, whereas there are several important immunologic events that occur during an asymptomatic period leading up to the tissue destruction. Thus a biomarker that could identify patients with severe acute GVHD prior to the occurrence of symptoms could allow for earlier intensification of immunosuppressive therapy. This could interrupt the progression of the disease, potentially decreasing morbidity and mortality. To that end, several groups have worked on identifying biomarkers of acute GVHD.

Paczesny *et al.* used an ELISA based approach to screen 120 distinct candidate proteins in the plasma of individuals with early signs of acute GVHD. This led to the discovery and validation of an ELISA panel composed of antibodies to 4 proteins (interleukin-2-receptor-alpha, tumor-necrosis-factor-

receptor-1, interleukin-8, and hepatocyte growth factor), which was able to detect acute GVHD with a specificity of 94%.[14] However, these results have limitations. Of particular importance is the fact that this study was conducted using plasma samples taken from patients who had already been diagnosed clinically. Thus these biomarkers are in fact confirmatory, not predictive. Furthermore, patients who had other complications of allogeneic hematopoietic stem cell transplantation such as veno-occlusive disease and sepsis were excluded from the study. Therefore, the specificity of this panel may be inflated. Other studies have been done using high throughput proteomic analysis of urine and serum, but they are similarly limited by the use of samples from patients who can already be diagnosed clinically with acute GVHD.[15-17]

One of the difficulties in identifying a biomarker of acute GVHD is determining potential sources of biomarkers. As already mentioned, previous studies have been done on plasma, serum and urine. Blood and blood components seem to be the most logical choice. But proteomic analysis of blood is inherently problematic since it contains such a large number of proteins, yet the majority of the proteome is composed of a small number of highly abundant proteins such as albumin and the immunoglobulins. In order to identify a protein biomarker of acute GVHD, it is necessary to first deplete the high abundance proteins, and focus on a more specific source of potential biomarkers. Plasma exosomes may offer a way to do just that.

II. Historical Significance of Exosomes

The discovery of plasma exosomes dates back to the late 1960s. At that time, Wolf *et al.* published results which demonstrated that the coagulation of platelet-depleted plasma was due to lipid-rich microparticles produced by platelets. They showed that the coagulability of platelet-depleted plasma was eliminated when these microparticles were removed by ultracentrifugation.[18] Furthermore, they demonstrated by electron microscopy the extrusion of these particles from intact platelets, and they reported finding platelet-specific components in the microparticles themselves.[18] Unfortunately, the significance of their findings was almost entirely overlooked at the time.

The next time that exosomes appeared in the cell biology literature was in the 1980s, when a group at McGill University observed them in the media of cultured reticulocytes.[19, 20] At this time, it was already established that reticulocytes lose their transferrin receptors as they mature into erythrocytes, and it had been assumed that this was due to receptor internalization and lysosomal degradation. However, over the course of several years, this group reported findings which described a novel mode of transferrin receptor loss.[21-24] They demonstrated that the transferrin receptor is selectively externalized via secretion of exosomes (see Figure 1).

The work of Johnstone's group in Montreal made it clear that the production of exosomes was not unique to platelets. It also shed light on the fact that exosomes have a variety of functions, and that these functions depend on the cell which produced them. However, it was more than a decade after Johnstone et al's seminal publication that exosomes really began to attract interest in other fields.

In the mid to late 1990s, it was discovered that exosomes were involved in many aspects of immunobiology. This led to a surge in research oriented toward exploring their involvement in the immune response, and tumor immunology in particular. Several years later, exosome research evolved yet again, this time to encompass the search for biomarkers of disease.

III. Exosome Biogenesis

The work of Johnstone *et al.* significantly impacted our understanding of the process by which exosomes are formed. They described the basic steps of exosome formation and release, which are depicted in Figure 2.[22] The first step is simple endocytosis. The plasma membrane invaginates and pinches off,

Figure 1

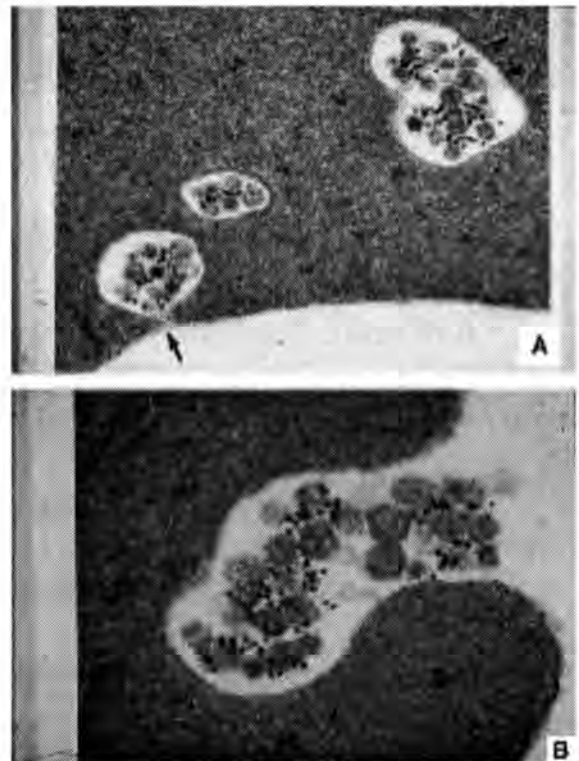


Figure 1. Exosomes in maturing sheep reticulocytes. (A) Immunogold labeling of transferrin receptor after 18 hour incubation. The gold label is located in the multivesicular body, on the intraluminal vesicles. (B) After 36 hour incubation, it can be seen that the multivesicular body fuses with the plasma membrane, extruding the vesicles (exosomes). Taken from Ref [21].

generating an endocytic vesicle. Thus, the orientation of membrane proteins is inverted, with the extracellular components on the inside of the vesicle and the cytosolic components on the exterior. This vesicle fuses with the early endosome. Next, as the endosome matures, its membrane invaginates and buds inwardly, producing an intraluminal vesicle. After the inward budding process has occurred multiple times, the endosome is filled with numerous intraluminal vesicles, and it is now called the multivesicular body. Importantly, the process by which these vesicles are formed results in the membrane proteins having the same orientation that they had in the plasma membrane. The intraluminal vesicles are nascent exosomes, which are not released until the membrane of the multivesicular body fuses with the plasma membrane in a manner similar to exocytosis. There are three salient points that can be taken away from their discoveries regarding exosome biogenesis. Firstly, the orientation of exosomal membrane proteins recapitulates that of the cell of origin. Therefore, they harbor ligands able to bind extracellular receptors. Secondly, during the invagination of the endosome, exosomes actually engulf cytosolic components, such as proteins and RNA. This makes them an ideal source of biomarkers. Finally, it must be noted that this model left many unanswered questions. Most importantly, it did not explain how proteins are actually sorted into exosomes. While there are still significant gaps in our understanding of the process by which proteins are sorted into the intraluminal vesicles of the multivesicular body, much can be said about this topic.

Figure 2

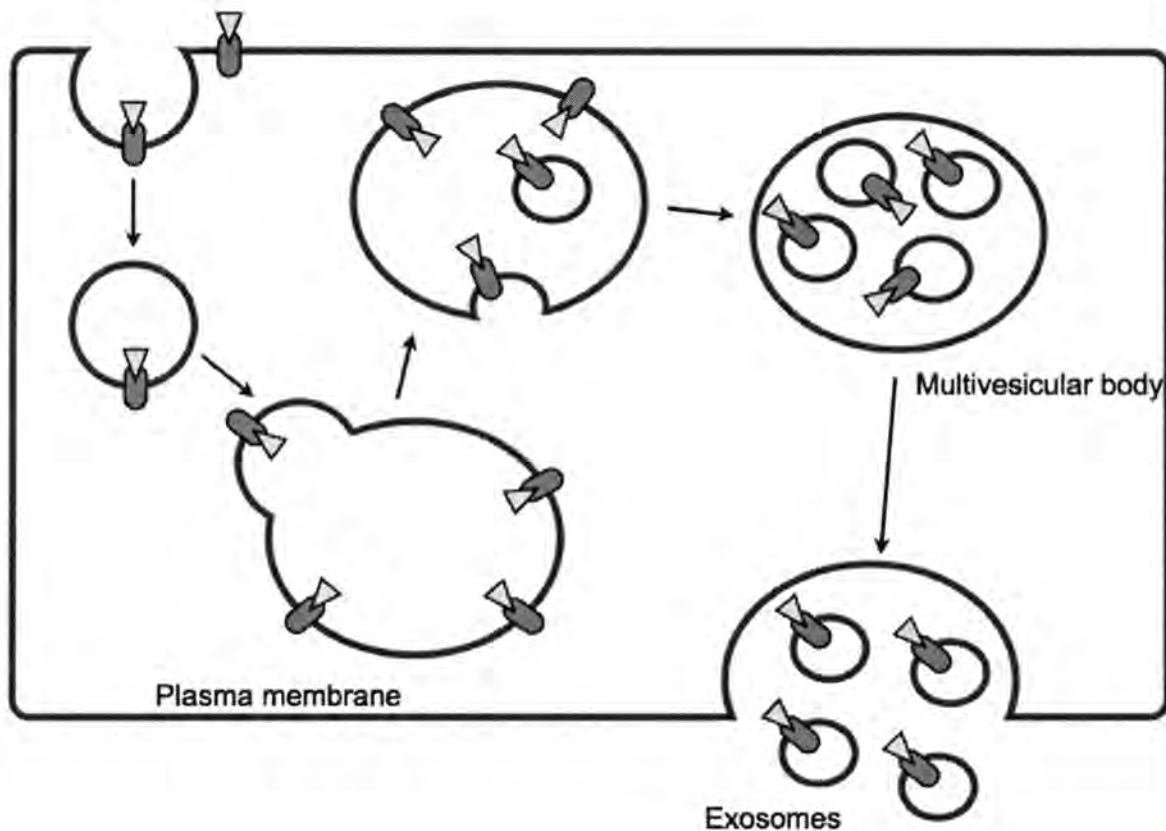


Figure 2. This is a pictorial representation of exosome biogenesis. The orientation of the plasma membrane protein (e.g. transferrin) is of particular importance. Note that in the exosomes, it is the same as in the original plasma membrane.

Ubiquitination is a key event in protein degradation. It targets proteins for both proteasomal and lysosomal degradation. In the latter, ubiquitinated membrane proteins that are endocytosed are sorted into intraluminal vesicles as the endosome matures into a multivesicular body.[25] The ESCRT (endosomal sorting complex required for transport) complex is crucial to this process. It has ubiquitin binding domains, which allow it to attach to the ubiquitinated proteins. Then, once invagination occurs, it catalyzes the scission of the endosomal membrane, resulting in interior budding.[25-27] Having said that, it is important to note that this is not the only way that proteins can be sorted into intraluminal

vesicles. For example, it has been shown that some proteins, including the transferrin receptor are capable of independent interaction with the ESCRT complex.[28] Additionally, some proteins can be sorted into the intraluminal vesicles by ESCRT-independent mechanisms. For example, tetraspanins (e.g. CD63, CD81) can partition into lipid microdomains.[29] In conclusion, the sorting of proteins into intraluminal vesicles is a complex process, which is only beginning to be described.

IV. The Immunobiology of Exosomes

Acute Graft-Versus-Host disease (GVHD) occurs following allogeneic hematopoietic stem cell transplantation. Briefly, antigen presenting cells (APCs), of which dendritic cells are the most important, take up alloantigens that have been liberated during tissue damage. The APCs process these antigens and present them in an MHC-dependent manner to T lymphocytes. Following antigen recognition, clonal expansion of T and B cells occurs, generating a population of cells which are reactive to the transplant recipient's alloantigens. These cells cause massive damage to a variety of host tissues. The primary mediator of tissue damage in acute GVHD is the cytotoxic T lymphocyte. In summary, the most important cell types in the pathophysiology of acute GVHD are the dendritic cell, the B lymphocyte the helper T lymphocyte, and the cytotoxic T lymphocyte. Exosomes produced by the cells of the immune system have been reviewed elsewhere.[30] However, it is particularly important to note that dendritic cells, B lymphocytes, and cytotoxic T lymphocytes are known to produce exosomes, and that these exosomes are functional. Therefore, since

these are hematologic cells, plasma exosomes are an attractive source for acute GVHD biomarker discovery.

T lymphocytes

Current research has focused primarily on the effects of exosomes derived from other cells on T lymphocytes, and consequently little work has been done on exosomes derived from T lymphocytes themselves. In fact, of all the leukocytes, exosomes derived from T lymphocytes have been studied the least. However, there is evidence to suggest that exosomes released by cytotoxic T lymphocytes play a role in sending the “lethal hit” to target cells.

CD8+ Cytotoxic T lymphocytes contain an organelle called the cytolytic granule. Originally, it was thought that the cytolytic granule contained soluble forms of the cytolytic molecules released by cytotoxic T lymphocytes to deliver the lethal hit to target cells. However, Peters *et al.* demonstrated that the cytolytic granule contains vesicles which are secreted, and that these vesicles contained perforin and granzyme, cytotoxic molecules crucial to the function of cytotoxic T lymphocytes. Additionally, they showed that the vesicles contained the T cell receptor, CD8 and CD3.[31-33] While these vesicles were not specifically called exosomes, it is now clear that they share many of the characteristics of exosomes. For example, Peters' group found that the delimiting membrane of the cytolytic granule was enriched in CD63 and LAMP-1 (CD9), both well-known markers of exosomes.[34] It is not a great logical leap to hypothesize that these proteins would be present in the vesicles within the cytolytic granule as well, since they are derived from the cytolytic granule itself.

In fact, a more recent study found CD63 enrichment in vesicles produced by activated cytotoxic T lymphocytes. Furthermore, this study demonstrated that cytotoxic T lymphocytes secrete these vesicles in response to activation via the T cell receptor (TcR), and that the vesicles themselves contain the TcR/CD3/zeta complex.[35] Therefore, it is reasonable to hypothesize that exosomes could have an important role in targeting specific cells during the delivery of the lethal hit.

B lymphocytes

B lymphocytes recognize specific antigens via the B cell receptor (BcR), which is an IgM or IgD molecule that is inserted into the plasma membrane. When the BcR recognizes its antigen, the B lymphocyte is activated and eventually transforms into a plasma cell, with the help of CD4+ T lymphocytes. The plasma cell produces antibodies and is consequently the effector cell of humoral immunity. In addition to this function, B lymphocytes can also function as antigen-presenting cells. It appears that the secretion of exosomes are implicated in this process.

Antigen primed B lymphocytes, but not resting B lymphocytes are capable of exosome secretion, and secretion is stimulated by interaction with activated T lymphocytes.[36] A recent study showed that culturing of B lymphocytes with an stimulatory anti-CD40 monoclonal antibody resulted in abundant secretion of exosomes.[37] However, it has not yet been proven that this is the mechanism by which activated CD4+ T lymphocytes effectuate exosome secretion by B lymphocytes. Exosomes secreted by B lymphocytes contain MHC-II-peptide

complexes (pMHC-II), and they are enriched in surface immunoglobulins, predominantly IgM.[37, 38]

As the presence of pMHC-II complexes implies, B lymphocyte derived exosomes have an immunomodulatory function. They are capable of stimulating clonal expansion of T lymphocytes which recognize the pMHC-II present on the surface of the exosomes.[38] However, more recent results suggest that this effect may not be seen in naive T lymphocytes, but only after they have been primed.[36] Their ability to stimulate activated T cells is an interesting finding, considering that follicular dendritic cells are known to adsorb exosomes containing pMHC-II.[39] Thus B lymphocytes in the lymph node may stimulate T lymphocytes in this indirect mechanism (although it is also plausible that these pMHC-II carrying vesicles are derived from dendritic cells). Finally, since CD40L appears to stimulate the secretion of exosomes with large amounts of the surface immunoglobulins IgM and IgD, it is possible that exosomes serve as an alternative means of degrading surface immunoglobulins during class switching. This function would be analogous to the function of exosomes as a means for maturing reticulocytes to externalize the transferrin receptor. Having said all that, the *in vivo* function of B lymphocyte derived exosomes remains unclear since most of the studies performed on B lymphocyte derived exosomes were done *in vitro*.

Dendritic Cell Derived Exosomes

Dendritic cells are the major antigen-presenting cells of the immune system. They phagocytose antigens, process them, and present them as pMHC-II

complexes to helper T cells, cytotoxic T lymphocytes and B lymphocytes. Thus, dendritic cells play a central role in the immune response. Dendritic cell-derived exosomes may as well. For example, *in vivo* studies have shown that exosomes derived from cultured dendritic cells that have been previously pulsed with an antigen are capable of generating a specific immune response to that antigen when they are transferred to an unexposed animal. This has been demonstrated both prophylactically, as in a study which used dendritic cell derived exosomes to protect from congenital *Toxoplasma gondii* infection in mice, and therapeutically, as shown in a study using dendritic cell-derived exosomes to generate an immune response to existing tumors in a mouse model.[40-42] Despite these and other results, the immunomodulatory effects of dendritic cell derived exosomes are only beginning to be elucidated. However, two salient facts are evident at this point. First, dendritic cell derived exosomes exert their immunomodulatory effects predominantly indirectly, via interactions with bystander cells of the immune system. Secondly, the maturation status of the dendritic cell of origin has a profound influence on the immunomodulatory effects of the exosomes that it secretes.

A pertinent example of the former is indirect activation of the immune system, in which dendritic cell derived exosomes elicit an immune response through interaction with bystander dendritic cells. Early experiments showed that exosomes derived from immature dendritic cells were able to stimulate naive CD4⁺ T cell activation and proliferation both *in vitro* and *in vivo*. However, their immunogenicity required the presence of mature dendritic cells; it was later

proven that the exosomes transferred functional pMHC-II complexes to bystander mature dendritic cells, which in turn stimulated CD4+ specific to that antigen.[43] Similarly, later work demonstrated that immature dendritic cell derived exosomes were capable of transferring functional pMHC-I complexes to mature dendritic cells *in vitro* and *in vivo*, and that this resulted in a cytotoxic T lymphocyte response against the melanoma antigen MART-1.[44] In summary, it appears that dendritic cell derived exosomes are capable of loading mature dendritic cells with specific pMHC complexes, which direct the immune response against a specific antigen.

Since it was clear that the transfer of pMHC complexes from dendritic cell derived exosomes to bystander dendritic cells was the basis for their functionality as immunomodulators, several studies were then conducted to elucidate the mechanism of transfer. First, it was discovered that ICAM-1 was necessary for bystander dendritic cells to bind to dendritic cell derived exosomes.[45] Later on, it was demonstrated that dendritic cells use LFA-1 to bind to exosomes.[46] Thus it is now clear that LFA-1/ICAM-1 binding is the mechanism by which exosomes are bound by bystander dendritic cells. Interestingly, these studies also showed that internalization and processing of the exosomes by the dendritic cells was not required for the elicitation of an immune response, although this does not exclude it from occurring.

A relevant criticism of the work done on the mechanism of exosome uptake by bystander APCs is that they were done using exosomes derived from mature dendritic cells, whereas the previous work demonstrating transfer of pMHC

complexes to bystander cells was done with exosomes derived from immature dendritic cells. Thus it has not been confirmed that LFA-1/ICAM-1 binding is the mechanism by which immature dendritic cell derived exosomes are taken up by bystander dendritic cells. But inference from the evidence below suggests that this is case. Furthermore, the knowledge that LFA-1/ICAM-1 binding mediates the interaction of dendritic cell exosomes with bystander cells demands investigation of the possibility of their interaction with cell types other than dendritic cells.

It is well-known that T lymphocytes have LFA-1 on their plasma membrane as well. Therefore it is reasonable to hypothesize that they too could bind to exosomes derived from dendritic cells. In fact a recent study demonstrated that CD4+ T lymphocytes use LFA-1 to take up exosomes derived from immature dendritic cells and that this results in transfer of MHC-II from exosomes to the T cells.[47] Interestingly, only activated T lymphocytes were able to do so. This selectivity may be explained by the fact that LFA-1 undergoes a conformational change when the T lymphocyte transitions from the resting state to the activated state.[47] These results are significant because they demonstrate the uptake of immature dendritic cell derived exosomes by bystander cells using the same mechanism as previously described for mature dendritic cell derived exosomes. In this case, the bystander cells were activated T lymphocytes, not dendritic cells. Nevertheless, in addition to demonstrating a novel interaction between dendritic cells and activated T lymphocytes, it lends credence to the hypothesis that bystander dendritic cells also bind immature dendritic cell derived exosomes

using LFA-1. Additionally, this is possibly the mechanism by which all cells bind to dendritic cell derived exosomes. Furthermore, these results underscore the complexity of the immunomodulatory effects of dendritic cell derived exosomes.

The ability of activated T lymphocytes to bind to and take up exosomes significantly increases the complexity of the immunomodulatory effects of dendritic cell derived exosomes, because it results in the conversion of these cells into antigen-presenting cells. For example, activated CD4⁺ T lymphocytes which have taken up exosomes derived from mature dendritic cells are capable of stimulating a CD8⁺ response both *in vitro* and *in vivo*.^[48] Furthermore, the findings of Nolte-'t Hoen et al suggest that it may be possible for dendritic cell derived exosomes to directly stimulate an immune response. In fact, it has been demonstrated that exosomes derived from immature dendritic cells are capable of directly inducing *in vitro* IFN-gamma production (a marker of activation) by CD8⁺ T lymphocytes isolated from human peripheral blood.^[49] Conversely, it is possible that the presentation of pMHC complexes from immature dendritic cell derived exosomes by CD4⁺ T lymphocytes could lead to downregulation of the immune response, although this has not yet been demonstrated experimentally.^[47, 50] Therefore, it is clear that at least part of the immunomodulatory effect of dendritic cell derived exosomes is mediated by interaction with activated T cells and this must be accounted for in future work.

The clinical potential of dendritic cell derived exosomes is only beginning to be investigated. In 2005, two papers were published describing the first attempts to use dendritic cell derived exosomes in tumor vaccines. In short, exosomes

derived from autologous monocyte derived immature dendritic cells were administered in four weekly subcutaneous/intradermal injections to patients with either advanced melanoma or advanced non-small cell lung cancer.[51, 52] These phase I clinical trials demonstrated the feasibility of large scale production of dendritic cell derived exosomes, and that their administration resulted in very limited toxicity. However, while taking into consideration that these trials were not designed to measure efficacy, it is noteworthy that the data from these trials do not seem to indicate that vaccination with immature dendritic cell derived exosomes is capable of eliciting a cellular response leading to tumor eradication. Of the 24 patients included in these trials, only one demonstrated CD8+ reactivity to tumor antigens. Interestingly, some patients did respond to therapy, and their response was due increased natural killer (NK) cell activity. Therefore, the results of these trials generated some important questions regarding the efficacy of dendritic cell derived exosome therapy as cancer immunotherapy and its mechanism of action.

The results of these clinical trials necessitated investigation of the mechanism by which immature dendritic cell derived exosomes effectuate increased NK cell activity. Subsequent work has shed some light on this new area of exosome research. In brief, exosomes derived from immature dendritic cells harbor ligands which bind the activating receptor NKG2D on the NK cell membrane. They also contain BAT-3, a pro-apoptotic protein, which is a ligand for the natural cytotoxicity receptor NKp30.[53, 54] Finally, immature dendritic cell derived exosomes have IL-15 receptor alpha, which allows them to bind

soluble IL-15 and trans-present it to NK cells, thereby activating them.[53]

Combined, these results demonstrate that immature dendritic cell derived exosomes are powerful stimulators of NK cell activity. This potential could be utilized to increase their efficacy as inducers of tumor immunity.

The lack of a cellular response observed in these trials is paradoxical, but may be explained by the fact that both of these trials used exosomes derived from immature dendritic cells. While it is true that both immature and mature dendritic cells secrete exosomes, there are marked differences between the two. First, immature dendritic cells secrete 2-3 fold more exosomes than mature dendritic cells.[45] Conversely, exosomes derived from mature dendritic cells are 50-100 fold more efficient at inducing activation and proliferation of naive CD4+ T cells *in vitro* and *in vivo*. [45] The disparity in immunogenicity is likely explained by differences in the amounts of MHC and costimulatory molecules. Specifically, exosomes derived from mature dendritic cells had higher amounts of ICAM-1, CD86, 2-3 times more MHC-II, and 1.5 times more pMHC-II complexes in comparison to immature dendritic cells. In contrast, exosomes derived from immature dendritic cells had increased amounts of MFG-E8 and slightly more MHC-I.[45] It is important to note that low amounts of costimulatory molecules found in immature dendritic cell derived exosomes could result in T cell anergy and downregulation of the immune response. In fact, a recent study demonstrated that immature dendritic cell derived exosomes were capable of mitigating cardiac allograft rejection in a rat model, suggesting that they may have tolerogenic qualities.[55] Therefore, there is a need for the systematic

comparison of the *in vivo* effects of exosomes derived from immature dendritic cells and those derived from mature dendritic cells.

The final element of research on dendritic cell derived exosomes is the use of combination pharmaceutical agents and dendritic cell derived exosomes. This is a relatively new concept, but preliminary evidence indicates that it could be a clinically useful avenue to explore. A good example of the interaction of these two therapies is seen in the cardiac allograft study that was previously cited. In that particular study, immature dendritic cell derived exosomes alone delayed MHC-mismatched cardiac allograft rejection in a rat model.[55] However, a later study by that same group demonstrated the effects of the combination of immature dendritic cell derived exosomes with LF15-019, a novel NF- κ B inhibitor that is a known tolerogen. Combination of the two was shown to induce long-term tolerance.[55] Synergy between exosome therapy and pharmacologic immunomodulators has also been observed elsewhere. Specifically, it has been demonstrated that coadministration of pathogen-associated molecular pattern molecules (PAMPs), which induce dendritic cell maturation *in vivo*, with dendritic cell derived exosomes in tumor vaccination is superior to vaccination with exosomes alone.[57, 58] Additionally, cyclophosphamide, which is known to inhibit regulatory T lymphocyte activity, has been shown to improve tumor rejection when administered in combination with dendritic cell derived exosomes.[58-60] Thus the combination of immunomodulators with dendritic cell derived exosomes may be able increase

their efficacy. This will be an important component of future exosome immunotherapy research.

The preponderance of evidence shows that dendritic cell derived exosomes are powerful immunomodulators. They harbor functional peptide-MHC complexes, and are capable of eliciting an immune response either through direct stimulation of MHC-restricted T lymphocytes, or, more commonly, indirectly through the transfer of pMHC complexes to bystander antigen-presenting cells. They are also able to stimulate NK cell activity, and their immunomodulatory effects are synergistic with pharmacotherapy. In the future, dendritic cell derived exosomes may be clinically useful tool in cancer immunotherapy, as well as other forms of immunotherapy.

V. Exosomes and Biomarker Discovery

As previously stated, exosomes contain specific components derived from the cell of origin. Furthermore, they are readily isolated from many biological fluids. The following table lists some of the recent advances in biomarker discovery using exosomes. Table 1 is a list of recently published papers in the field of exosome-based biomarker discovery. Complete bibliographic information may be found in the list of references on page 59. [61-69] It is clear that others have had significant success identifying biomarkers associated with exosomes. Given their results, and the data which demonstrate a role for exosomes in immunomodulation, we hypothesized that proteomic profiling of plasma exosomes would yield a potential biomarker of acute GVHD.

Table 1. Recent Publications in Exosome-Based Biomarker Discovery[61-69]

Title	First Author	Journal and Year	Biological Fluid	Results
Nucleic acids within urinary exosomes/microvesicles are potential markers for renal disease	Miranda KC	Kidney International; April 2010	urine	urinary exosomes contain RNA profile (including rRNA, miRNA, and mRNA) similar to that of kidney tissue
Detection of microRNA expression in human peripheral blood microvesicles	Hunter M	PLoS One 2008	blood	miRNA was isolated from plasma exosomes of normal subjects
MicroRNA signatures of tumor-derived exosomes as diagnostic biomarkers of ovarian cancer	Taylor DD	Gynecologic Oncology 2008	blood	miRNA profiles of tumor derived plasma exosomes were found to be similar to tumor tissue. Exosomes are therefore potential surrogates for obtaining biomarkers.
Urinary exosomal transcription factors, a new class of biomarkers for renal disease	Zhou H	Kidney International; Sept 2008	urine	The transcription factors ATF3 and WT-1 were found to be elevated in urine exosomes in animal models and human patients with acute kidney injury and focal segmental glomerulosclerosis, respectively.
Exosomes from human saliva as a source of microRNA biomarkers	Michael A	Oral Disease; Jan 2010	saliva	miRNA was isolated from salivary exosomes of normal subjects and a patient with Sjogren syndrome
Exosomal microRNA: a diagnostic marker for lung cancer	Rabinowitz G	Clinical Lung Cancer; Jan 2009	blood	Exosomal small RNA and miRNA were isolated from patients with adenocarcinoma and compared to controls

Proteomic analysis of human parotid gland exosomes by multidimensional protein identification technology (MudPIT)	Gonzalez-Begne M	Journal of Proteome Research; 2009	saliva	Described the proteome of human parotid gland exosomes. Notably, they show that a large number of proteins are cytosolic in origin.
High levels of exosomes expressed CD63 and caveolin-1 in plasma of melanoma patients	Logozzi M	PLoS One; 2009	plasma	This paper describes a novel method for the isolation of melanoma exosomes from plasma. These exosomes contain the melanoma marker caveolin-1.
Claudin-containing exosomes in peripheral circulation of women with ovarian cancer	Li J	BMC Cancer; 2009	blood	Claudin-4 was found in plasma exosome of women with ovarian cancer. It had a 51% sensitivity and 98% specificity.
Identification and proteomic profiling of exosomes in human urine	Pisitkun T	Proceedings of the National Academy of Sciences; 2004	urine	Exosomes were isolated from human urine. Known biomarkers of renal and systemic diseases were found in the exosomes, indicating that urinary exosomes might be a source of further biomarkers.

Methods

I. Protocol Development

In order to discover plasma exosome-associated biomarkers of acute GVHD, we first had to develop a protocol for the isolation of exosomes from cryopreserved plasma. We chose to use a method of differential centrifugation. To validate the presence of exosomes in the final pellet, we probed for known exosome markers by Western blot, and we examined the pellet by electron microscopy.

I.a Differential Centrifugation of Cryopreserved Plasma

Plasma samples were thawed in a 37°C water bath. Samples were then transferred to 15ml Falcon tubes and diluted to 10% plasma by adding 25.8ml of 1x PBS and 1.2ml of 25x Roche mini-complete EDTA-free protease inhibitor cocktail (each sample was divided in half). Samples were spun at 1,000xg at 4°C for 5 minutes, to remove any macroparticulate. Supernatant was transferred to clean tubes and centrifuged for 20 minutes at 17,000xg at 4°C. Supernatant from this spin was transferred to clean 50ml Falcon tubes and filtered through at 0.22um filter (Steriflip). Filtered supernatant was then centrifuged for 1 hour at 200,000xg at 4°C. Supernatant was removed and pellets were washed and resuspended in 1ml of 1xPBS. Resuspended pellets were transferred to 1.5ml Beckman ultracentrifuge tubes and centrifuged for 1 hour at 186,000xg at 4°C.

Supernatant was aspirated and discarded and the pellets were used for proteomic analysis.

I.b Extraction of Protein from Exosome Pellets

Proteins were solubilized from the pellet by adding 250ul of homemade resolubilization buffer (100ul 1.0M Tris-HCl, pH7.4, 20ul of 0.5M EDTA, 2.4g urea, 50ul of 0.005% Triton X-100, 100ul of 10% SDS, 100ul of 100x Calbiochem protease inhibitor cocktail, and ddH₂O to a final volume of 10ml) to each pellet, followed by vigorous pipetting. Solubilized proteins were then precipitated using trichloroacetic acid (TCA) and acetone. Briefly, 32ul of 100% TCA was added to each 250ul sample and vortexed for about 5min (final concentration of TCA was 11%). Samples were incubated for 1 hour at 4°C. Then, each tube was filled to the top with ice cold acetone (approximately 1.2ml of acetone was added) and briefly vortexed. Samples were then incubated overnight at -20°C. The next morning, samples were centrifuged at 20,000xg at 0°C for 20 minutes, to pellet the protein. Supernatant was aspirated and pellet was washed 4 times with ice cold acetone. Acetone washes were done by adding 1ml of fresh ice cold acetone, briefly vortexing the samples, and centrifuging them for 20 minutes at 20,000xg at 0°C. After the fourth wash, the acetone supernatant was aspirated and the pellets were dried in a vacuum dessicator. Protein pellets were redissolved using 50% DIGE no-salt buffer (3.5M urea, 1M thiourea, 2% CHAPS).

I.c Western Blotting of Exosome Markers

1D Gel and Membrane Transfer: 1D gel electrophoresis was performed using the Invitrogen NuPAGE system. Briefly, the sample was prepared so that it was 25% LDS sample buffer and 10% Reducing Agent. Samples were heated to

70°C for 10 min and sonicated in a water bath for 30 seconds. Samples were loaded into 4-12% Bis-Tris gels and gels were run for 45 minutes at 200V constant voltage using MOPS running buffer. Gels were removed and proteins were transferred to PVDF membranes using 100V constant voltage applied for 38 minutes.

Hsp70: PVDF membrane was blocked using 10ml of PBST (PBS 0.1% Tween) + 5% milk for 40 minutes at room temperature. Blocking solution was removed, and membrane was incubated for 1 hour at room temperature in 10ml of 1:5000 primary antibody (mouse anti-Hsp70; Abcam, ab6535, lot # 656321) in PBST +5% milk. The primary antibody was removed and membrane was washed 3 times, 10 minutes each, in PBST on an orbital shaker at room temperature. After washing, the membrane was incubated overnight at 4°C in 10ml 1:20,000 dilution of secondary antibody (goat anti-mouse HRP-conjugate, Abcam, ab7068, lot # 735618) in PBST +5% milk. The secondary antibody was removed, and the membrane was washed 3 times, 10 minutes each, in PBST and 1 time in PBS. The blot was incubated in WestPico ECL substrate for 4 minutes at room temperature and developed after 10 second exposure.

CD63: Eight µg of protein that had been extracted from the plasma exosome enriched pellet of a normal subject was used for this experiment. PVDF membrane was blocked using 10ml of blocking solution (PBST+5% milk) for 1 hour at room temperature. Blocking solution was removed, and the membrane was incubated for 1 hour at room temperature in 10ml of 1:1000 primary antibody (mouse anti-CD; Santa Cruz Biotechnology, sc-5275, lot #

J3108) in PBST+5% milk. The primary antibody was removed and the membrane was washed 3 times, 10 minutes each, in PBST on an orbital shaker at room temperature. After washing, the membrane was incubated at room temperature in 10ml 1:20,000 dilution of secondary antibody (goat anti-mouse HRP-conjugate, Abcam, ab7068, lot # 735618) in PBST+5% milk. The secondary antibody was removed, and the membrane was washed 3 times, 10 minutes each, in PBST and 1 time in PBS. The blot was incubated in Immobilon ECL substrate for 4 minutes at room temperature and developed after a 20 second exposure.

CD81: PVDF membrane was blocked using 10ml of PBST+5% milk for 1 hour at room temperature. Blocking solution was removed, and membrane was incubated for 1 hour at room temperature in 10ml of 1:1000 primary antibody (mouse anti-CD81; Abcam, ab79559, lot # F2205) in PBST+5% milk. The primary antibody was removed and the membrane was washed 3 times, 10 minutes each, in PBST on a shaker at room temperature. After washing, the membrane was incubated at room temperature in 10ml 1:20,000 dilution of secondary antibody (goat anti-mouse HRP-conjugate, Abcam, ab7068, lot # 735618) in PBST+5% milk. The secondary antibody was removed, and the membrane was washed 3 times, 10 minutes each, in PBST and 1 time in PBS. The blot was incubated in Immobilon ECL substrate for 4 minutes at room temperature and developed after 2 minute exposure.

Aquaporin 1 (AQP1): PVDF membrane was blocked using 10ml of PBST+5% milk for 70 minutes on orbital at room temperature. Blocking solution

was removed, and the membrane was incubated for 1 hour at room temperature in 10ml of 1:1000 primary antibody (mouse anti-AQP1; Santa Cruz Biotechnology, sc-32738, lot # F2205) in PBST+5% milk. The primary antibody was removed and membrane was washed 3 times, 10 minutes each, in PBST on a shaker at room temperature. After washing, the membrane was incubated at room temperature in 10ml 1:20,000 dilution of secondary antibody (goat anti-mouse HRP-conjugate, Abcam, ab7068, lot # 735618) in PBST+5% milk. The secondary antibody was removed, and the membrane was washed 3 times, 10 minutes each, in PBST and 1 time in PBS. The blot was incubated in Immobilon ECL substrate for 4 minutes at room temperature and developed after 2 minute exposure.

I.d Electron Microscopy

After isolation from plasma using the methods described in Section 1.a, 60ul of 2% paraformaldehyde was added to the pellet and it was shipped on ice overnight to the University of Montana's Electron Microscope Facility. A 5ul aliquot of the sample was placed on a Formvar-coated copper grid and allowed to bind for 30 minutes in a humidity chamber at room temperature. After binding the grids were rinsed with distilled water and stained with 1% Uranyl acetate for 10 minutes. The stain was wicked off and the grids were air-dried. The exosomes were imaged in a Hitachi H-7100 Transmission Electron Microscope at 75Kv.

II. Reproducibility Experiment

Large amounts of technical variability would cast significant doubt on the validity of any data generated using our protocol for the isolation of plasma

exosomes. We conducted the following experiment to assess the technical variability of the protocol.

II.a Samples

Blood was drawn simultaneously from 3 healthy volunteers into ACD-containing tubes. It was fractionated by centrifugation at 2,000xg 4°C for 10 minutes, and plasma was collected in 1.5ml tubes. Plasma was then flash frozen in liquid nitrogen and stored at -80°C overnight.

II.b Isolation of Exosomes from Plasma Samples

For this experiment, 3ml of plasma constituted a sample. One sample was used for subjects A and B, whereas 3 samples from subject C were used. All 5 samples were processed in parallel. Exosomes were isolated using the protocol previously described in Section I.a.

II.c Extraction of Proteins from Exosome Pellets

Protein was recovered from the plasma exosome-enriched pellets in the same way as described in Section I.b.

II.d Analysis of Samples

In addition to calculating the protein concentration of each sample, samples were analyzed by 1D gel electrophoresis and Western blot.

1D gel electrophoresis: Two 1D gels were run for this experiment. 1D gel electrophoresis was performed using the Invitrogen NuPAGE system. In short, 15ug of protein was used for each sample. The first gel contained protein samples obtained from plasma exosome pellets and supernatant from the 200,000xg spin, and the second gel contained protein samples obtained from

plasma exosome pellets and the plasma from which they were isolated. The appropriate volume of each sample was transferred to a 0.5ml tube. Then 5ul of Invitrogen NuPAGE LDS sample buffer and 2ul Invitrogen NuPAGE sample reducing agent were added to each sample. Total volume was brought to 20ul by adding milli-Q ddH₂O. The final concentrations of LDS sample buffer and reducing agent were 25% and 10%, respectively. Samples were heated for 10min at 70°C and sonicated for 30 seconds in a water bath. Samples were loaded onto 4-12% Bis-Tris 12 well gels. Gels were run for 45 minutes at 200V using MOPS running buffer. After the run was completed, the gel containing protein from plasma exosome pellets and plasma was stained with SyproRuby, and the gel containing protein from plasma exosome pellets and supernatant from 200,000xg spin was transferred to a PVDF membrane for Western blotting.

Protein Staining: The 1D gel containing protein from plasma exosome pellets and plasma from the above step was stained using the SyproRuby protein stain. Briefly, the gel was fixed for 30 min in a solution of 10% methanol 7% acetic acid on a shaker at room temperature. Fixative solution was removed and SyproRuby stain was added to the gel. The gel was incubated in SyproRuby overnight at room temperature on a shaker. Following staining, SyproRuby was removed and the gel was washed in 10% methanol 7% acetic acid for 30 minutes at room temperature. The gel was then washed for 10 minutes in milli-Q H₂O and imaged using a Bio-Rad Molecular Imager Fx and the software PD Quest.

Western Blotting: The gel was transferred to a PVDF membrane by using a constant voltage of 100V for 38 minutes. Following the transfer, the membrane

was put in 10ml of PBST+5% milk. Blocking was done at room temperature for 1 hour on an orbital. After 1 hour, the blocking solution was removed and the primary antibody, 10ml of 1:1000 dilution of mouse anti-CD81 (Abcam, ab59477-100, lot: 790975) in PBST+5% milk, was added. The primary antibody incubated overnight at 4°C on an orbital shaker. Primary antibody was removed, and the membrane was washed on a shaker at room temperature three times for 10 minutes each time in PBST. Following the washes, 10ml of the secondary antibody, 1:20,000 dilution of goat anti-mouse IgG conjugated with horse radish peroxidase (Abcam, ab7068-100, lot:735618) in PBST+5% milk was added to the membrane. After a 1 hour incubation at room temperature, the secondary antibody was removed, and the membrane was washed three times in PBST for 10 minutes each time. It was washed an additional time for 10 minutes in 1x PBS. Following the washes, the membrane was incubated for 3 minutes in the HRP substrate Immobilon (Millipore). The film of the blot was developed after 20 second exposure.

III. Acute GVHD Biomarker Discovery

III.a Samples

Seven 5ml frozen plasma samples were obtained from the Hollings Cancer Center Tissue Biorepository. These samples were collected on day 7 posttransplantation from patients who had undergone allogeneic hematopoietic stem cell transplantation at MUSC and consented to have deidentified samples collected for research purposes. Three of these patients developed severe acute Graft-Versus-Host disease (grades C and D) after the blood was obtained,

between 15 and 30 days posttransplantation. Four patients did not develop acute GVHD of any grade.

III.b Isolation of Exosomes from Plasma Samples

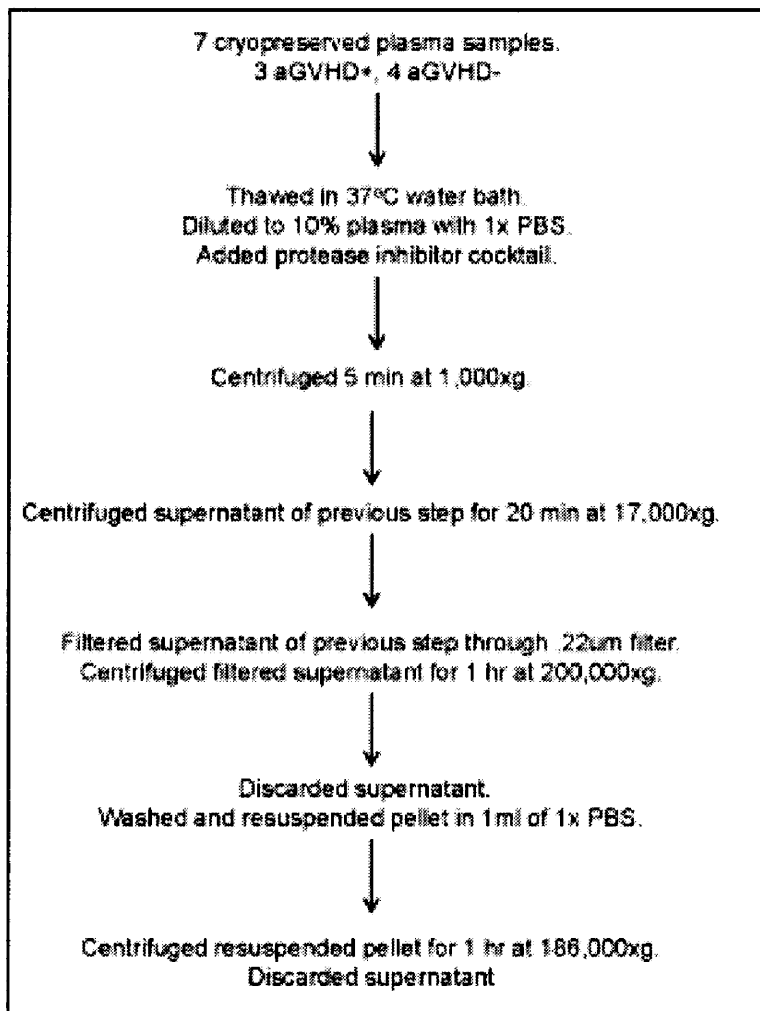
Exosomes were isolated from frozen plasma samples using the protocol previously described in Section 1.a. A flow chart of the methods is shown in Figure 3.

III.c Extraction of Protein from Exosome Pellets

Protein was recovered from the exosome-enriched pellets using the methods previously described in Section 1.b.

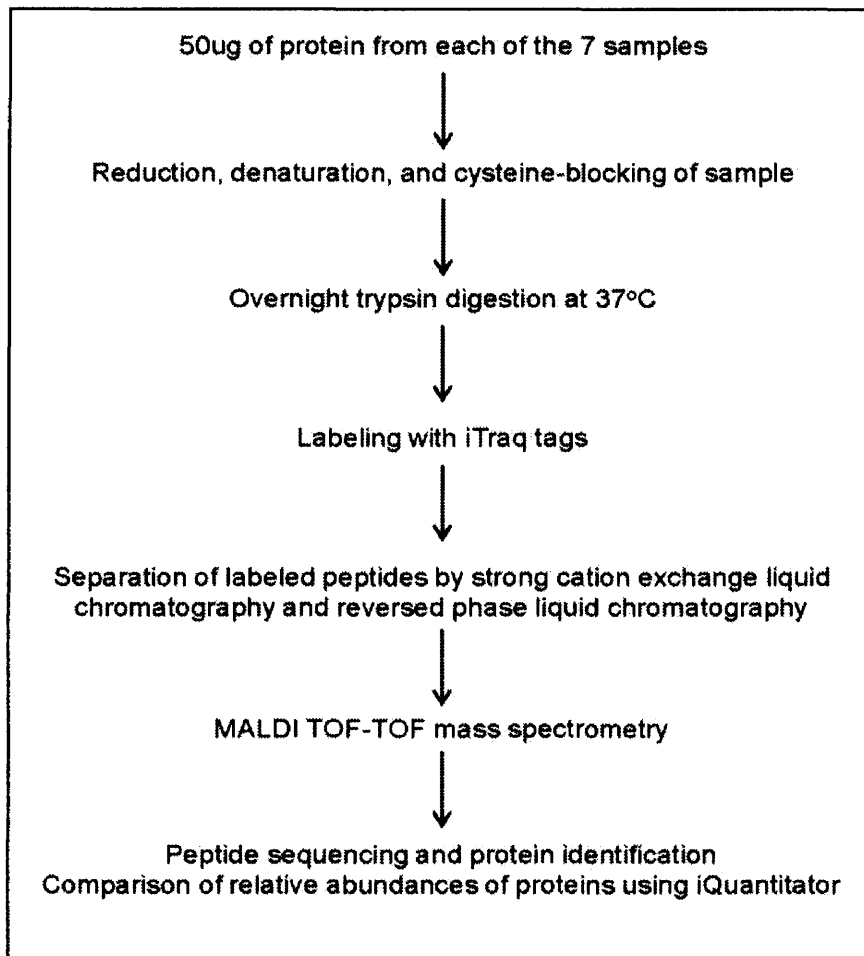
III.d Proteomic Analysis

Figure 3. Flow Chart of Exosome Isolation Protocol



Fifty ug of protein from each of the 7 pellets was analyzed by liquid chromatography mass spectrometry and relative abundance of peptides was computed using iTRAQ labeling (see Figure 4 for flow chart). The appropriate volume of each sample was transferred to a 0.5ml tubes. Then the appropriate volume

Figure 4. Flow Chart of Proteomics Methods



of 50% DIGE no-salt buffer was added to each to so that each sample had identical amounts of both protein and DIGE buffer. Next, the samples were diluted by adding 38.1 ul of iTRAQ dissolution buffer (0.5M triethylammonium bicarbonate, Applied Biosystems). This resulted in a final sample

volume of 46ul (see Table 2 for information on the contents of each sample before the iTRAQ protocol was performed). At this point, the samples were denatured and reduced by adding 1ul of denaturant (2%SDS) and 2ul of reducing agent (50 mM tris-(2- carboxyethyl)phosphine) from iTRAQ reagent kit (Applied Biosystems). Samples were incubated at 37°C for 1 hour. Next, 1ul of cysteine-blocking reagent (200 mM methyl methane- thiosulfonate (MMTS) in isopropanol, Applied Biosystems) was added to each sample and samples were incubated for 10 minutes at room temperature. Afterward, 10ul of trypsin (25 µg trypsin and 222 µg CaCl₂ dissolved in 25ul of milli-Q water) was added to each sample, and samples were vortexed and incubated overnight at 37°C. In order to ensure that the sample volume was under 50ul during the labeling step, samples were put in

a centrifugal vacuum concentrator for 20min following trypsin digestion. Then, because sample volume was below the optimal volume, 10ul of iTRAQ dissolution buffer was added to each sample, giving them a volume of 45ul. pH was measured to ensure that it was above 8 for the labeling reaction. Each vial of lyophilized iTRAQ label was reconstituted with 50ul of isopropanol and a vial was added to each sample. Samples were vortexed and incubated at room temperature in the dark for 2 hours. After labeling, the samples were combined into a single tube, put on dry ice, and shipped to Protea Biosciences, Inc in Morgantown, West Virginia. Protea Biosciences performed the liquid chromatography mass spectrometry according to the following protocol.

Strong Cation Exchange Liquid Chromatography (SCX LC)

The samples were fractionated using SCX ProteaTip SpinTips. Briefly, the tips were first washed to wet the packing material by adding 50µL of SCX loading buffer and centrifuging the system at 4000rpm for 2 min. The sample was then loaded in the spin tip and centrifuged at 4000rpm for 2 min after which it was washed to elute salts and other non-retained components by adding 50µL of the rinse solution (5mM ammonium formate in 10% acetonitrile) to the top of the SpinTip. The SpinTip was transferred to a new clean centrifuge tube to collect the sample during elution with 150µL of elution solution. Twelve different elution solutions were used to fractionate the peptides. They were 20, 40, 50, 60, 80, 100, 125, 150, 200, 250, 350, 500 mM ammonium formate in 10% acetonitrile. The collected fractions were cleaned by repeated lyophilizing and

reconstituting in a 0.1M acetic acid solution. After final lyophilization, the digests were reconstituted in LC run buffer and reversed phase LC was performed.

Table 2. Sample Composition for iTRAQ Study

Sample	acute GVHD Status	Sample Volume (ul of 50% DIGE buffer)	Added 50% DIGE buffer (ul)	Total Volume (ul)	iTRAQ Label
1	negative	5.87	2.02	46	113
2	positive	5.05	2.84	46	114
3	positive	5.9	1.99	46	115
4	negative	5.66	2.23	46	116
5	negative	5.1	2.79	46	117
6	negative	7.89	0	46	118
7	positive	6.11	1.78	46	119

* All samples had 38.1ul of iTRAQ dissolution buffer

Reversed Phase Chromatography and MALDI Mass Spectrometry

Reversed phase LC and MALDI TOF-TOF MS/MS mass spectrometry were done using an ABI Tempo LC MALDI mass spectrometer (ABI 4800 MALDI TOF/TOF). Briefly, digested and lyophilized sample fractions were reconstituted in 12 μ L of 0.1% TFA in diH₂O. 10ul of each sample fraction was injected onto the separation column (Merck Chromolith CapRod monolith column – 150 X 0.1mm). Each fraction was separated using the buffer gradient program listed in Table 3. As peptides eluted off the column, they were spotted onto a MALDI

plate. Matrix was spotted onto the target, and protein identification by MALDI TOF-TOF MS/MS was performed using the following parameters. The mass range used was 900-4000. 400 laser shots were fired per spectrum. The minimum signal to noise ratio (S/N) for MS acquisition was 10. The minimum S/N for MS/MS was 30. Each MALDI spot was interrogated until at least 4 peaks in the MS/MS spectra achieved a S/N of 70. Spectra were searched against the Uniprot-Swissprot database using the search engine Paragon and ABI ProteinPilot 3.0.

Table 3. Reversed Phase Gradient Program

Time/min	%A (0.1% acetic acid, 2% acetonitrile)	%B (0.1% acetic acid, 90% acetonitrile)
0	97	3
10	97	3
20	20	80
21	3	97
22	3	97
23	97	3
30	97	3

Results and Discussion

I. Protocol Development

At the beginning of our study, we did not have a protocol in place for the isolation of exosomes from cryopreserved human plasma. Accordingly, the first step was for us to develop such a protocol. We did so by searching the exosome literature, and by consulting with Dr. Viswanathan Palanisamy, an expert on exosomes here at the Medical University of South Carolina. Eventually, we settled on a protocol which involved the addition of a protease inhibitor cocktail to the plasma, dilution of the plasma with 1xPBS, and differential centrifugation. Hypothetically, this would result in a pellet enriched in exosomes. We sought to validate the presence of exosomes in the pellet by Western blot probing of known exosomal markers, and by visualization of the vesicles using electron microscopy.

I.a Validation of Exosomes in Pellet by Western Blot

In order to validate that exosomes were present in the pellet from the 200,000xg spin, we performed a series of Western blots on pellets obtained from different plasma samples of the same subject. Appropriate markers were chosen by consulting Exocarta, an online compendium of exosome research.

Figure 5. Western Blots of Exosome-Associated Proteins

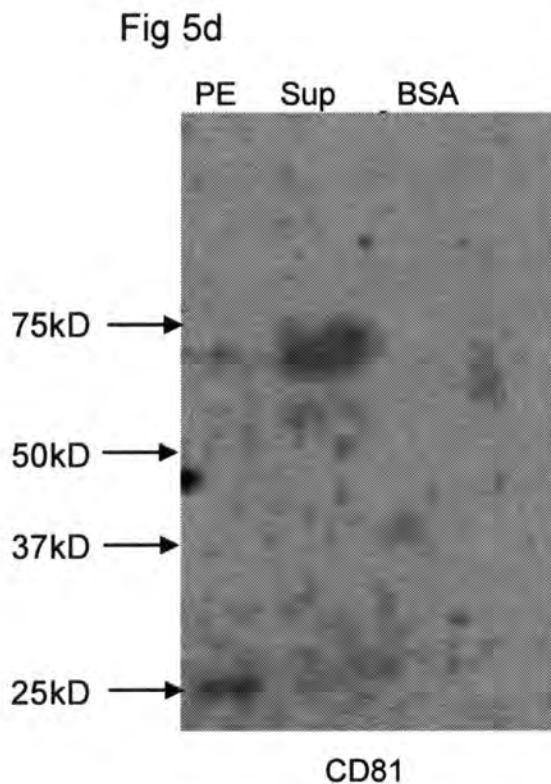
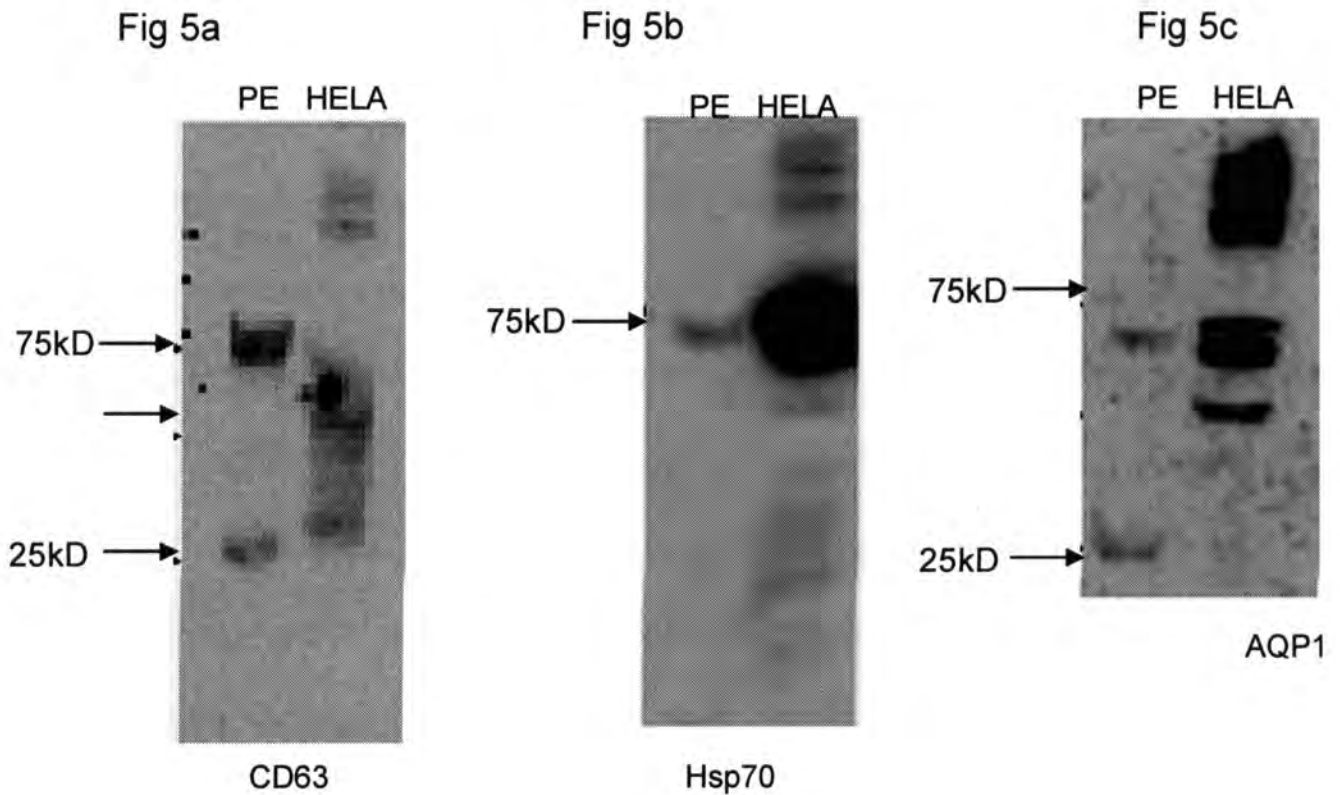


Figure 5 is a series of Western blots that were done to confirm the presence of exosomes in the final pellet that was obtained from frozen plasma. 8ug of protein was loaded into lanes of blot A. 15ug of protein was loaded in each lane for blots B, C and D. PE= plasma exosome pellet, HELA= HeLa cell lysate, Sup= 186,000xg supernatant, BSA= Bovine Serum Albumin. a) CD63 is a 30-60kD tetraspanin protein. HeLa cell lysate was a positive control. b) Hsp70 is 70kD protein. HeLa cell lysate was a positive control. c) AQP1 is a 26kD protein. HeLa cell lysate was a negative control. d) CD81 is a 26kD tetraspanin. BSA was a negative control, and the pellet was compared to supernatant from the spin from which it was isolated to show relative enrichment of the protein in the pellet.

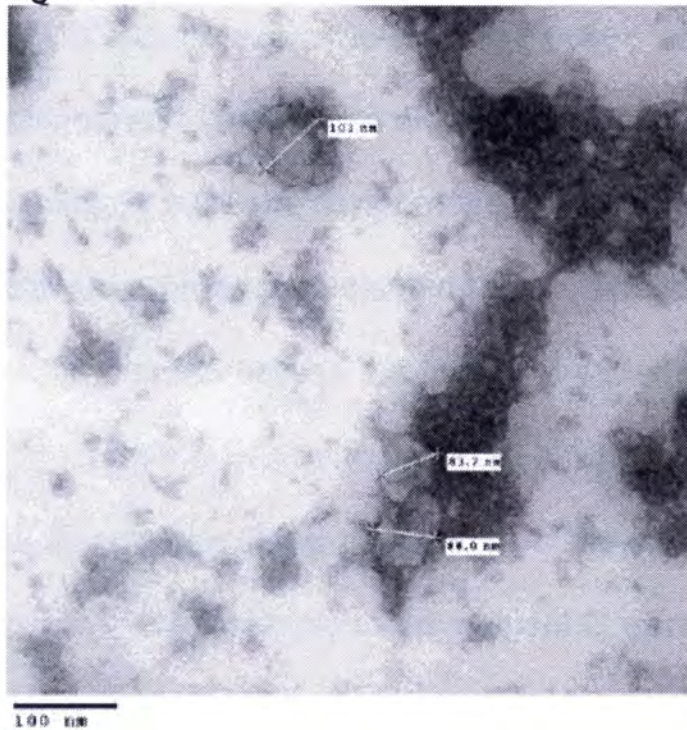
Specifically, we selected two of the proteins most commonly associated with exosomes, CD63 and CD81 as well as Hsp70 and AQP-1, a protein that is a component specific to plasma exosomes. See Figures 5a-d for results.

I.b Validation of Exosomes in Pellet by Electron Microscopy

While processing samples for Western blot analysis of exosome markers, we simultaneously processed a sample for analysis by electron microscopy. The images shown below (Figures 6a and b) show several membrane-bound vesicles that are in the same size range as exosomes, 40-100nm in diameter. This definitively proved that our protocol successfully isolated exosomes from cryopreserved plasma. However, as can be seen in these images, there is also a large amount of extraneous material surrounding the exosomes. Therefore, it is evident that our protocol did not lead to the isolation of pure exosomes.

Figure 6. Visualization of Plasma Exosomes by Transmission Electron Microscopy

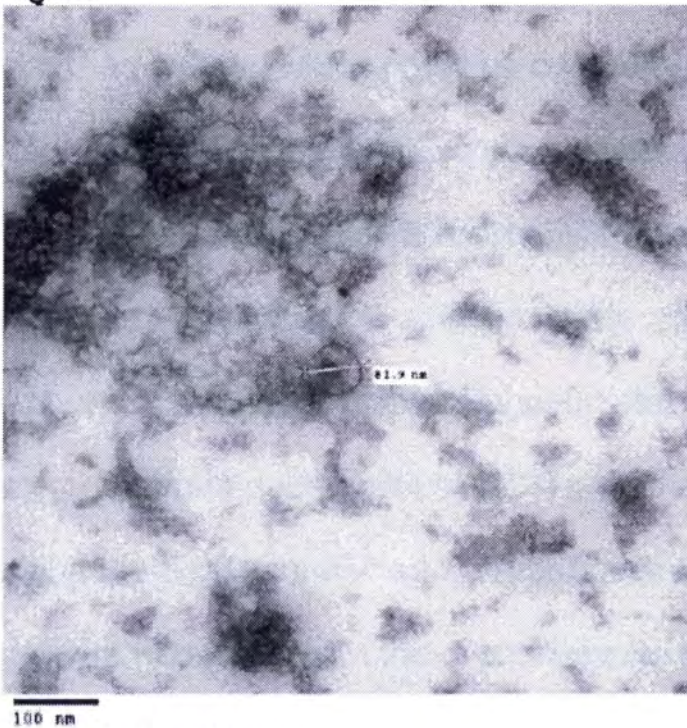
Fig 6a



100,000x magnification

Figure 6 shows exosomes isolated from the cryopreserved plasma of a normal subject. After isolation of the plasma exosome-enriched pellet, the pellet was fixed in 2% paraformaldehyde and shipped overnight to the University of Montana's Electron Microscope Facility.

Fig 6b



100,000x magnification

II. Reproducibility Experiment

The goal of our study is to identify differences in the abundance of proteins in the plasma exosome-enriched pellets of patients who developed acute GVHD compared to those who did not. Technical variability within the protocol could artificially increase or decrease protein abundances. Such variability would therefore produce misleading data. Therefore we designed the following experiment to assess the technical variability of our protocol.

Plasma was collected from 3 healthy volunteers. For this experiment, 3ml of plasma was used per sample. One sample was processed for subjects A and B, whereas 3 samples from subject C were used. All three of these samples were obtained at the same needle-stick. In all, five 3ml samples of plasma were used, and all samples were processed in parallel, according to the protocol described in the methods section. This resulted in five plasma exosome enriched pellets, which could be compared for the assessment of both biologic and technical variability. Comparison between subjects allowed for the assessment of biologic variability, whereas comparison of the triplicate samples obtained from subject C allowed for the assessment of technical variability.

After the final ultracentrifugation step (200,000xg spin), protein was extracted from each pellet by TCA-acetone precipitation and it was quantified using the BioRad modified Bradford assay. We determined the amount of protein recovered from the plasma exosome-enriched pellet of each sample. The data obtained from this assay are shown in Table 4. There was a large amount of variability in the overall protein yield when comparisons were made

Table 4

Sample Pellet	Total Protein (ug)	Protein per ml of plasma
A	78.51	26.17
B	113.33	37.78
C1	272.04	90.68
C2	297.91	99.3
C3	221.29	73.76

Table 4. This table shows the total protein extracted from the plasma exosome-enriched pellets isolated from 3 subjects. Intersubject comparison allows for the assessment of biologic variability. There are the samples from subject C, the comparison of which allows for assessment of technical variability.

from subject to subject. In contrast, when comparing the triplicate samples from subject C, there is much less variability. The mean total protein yield for subject C was 263.75ug. The standard deviation and standard error were 38.98 and 22.5, respectively. The coefficient of variation was 0.148.

This addressed the quantitative element of technical variability. The qualitative variability (that is the differences in the contents of the pellets) was assessed by 1D gel and Western blot. The 1D gel was stained with SyproRuby, a protein stain, following electrophoresis. This gel (Figure 7) compares the contents of 200,000xg pellets from each sample to plasma from the same sample, whereas the Western blot compares the pellets to supernatant from the 200,000xg spin, which pellets the exosomes down (again from the same sample). The 1D gel allows for the comparison of the content of the pellets. The Western blot does this as well, but it specifically allows for the demonstration of relative enrichment of CD81, an exosomal marker protein, in the pellet versus the supernatant. The 1D gel demonstrates that there is a marked difference in the banding pattern of 200,000xg pellets compared to plasma from the same sample. Compared to

Figure 7 Sypro Ruby Stain of 1D Gel

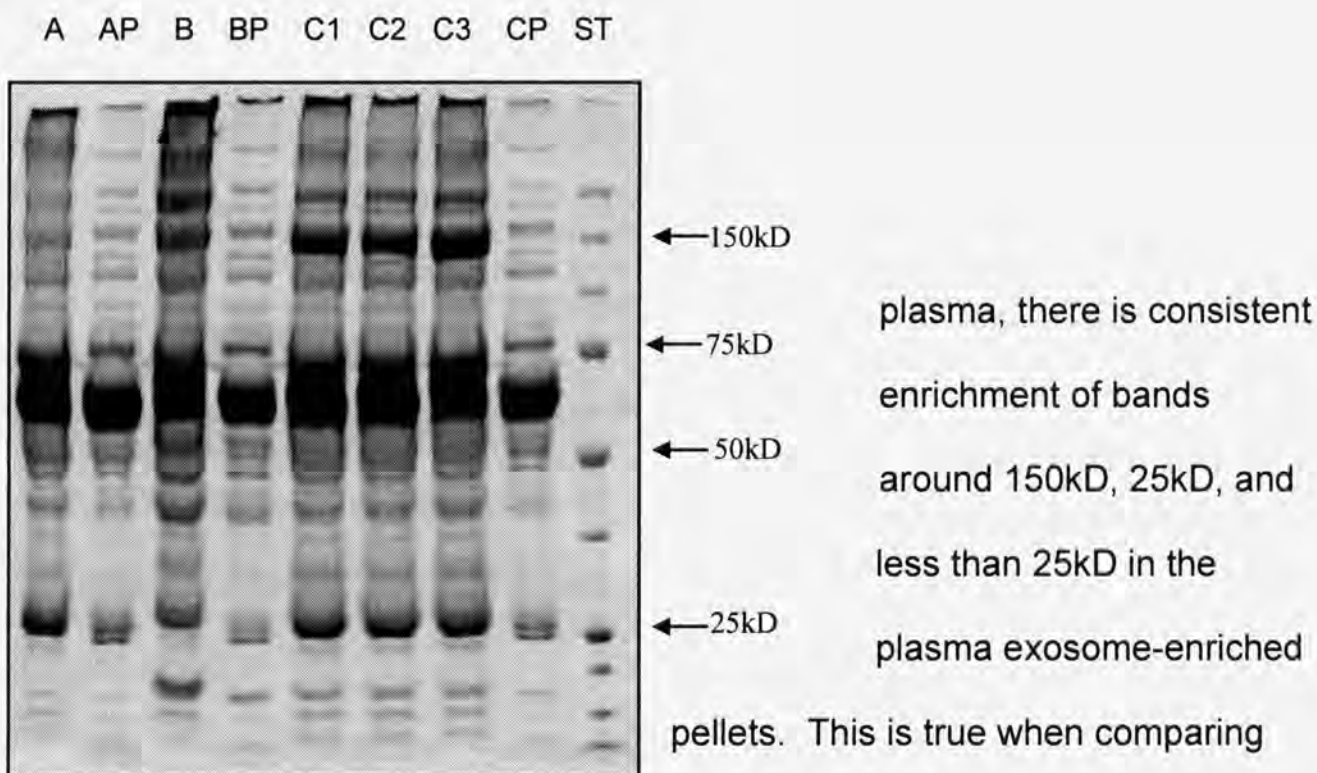


Figure 7

A, B C1, C2, and C3 designate lanes loaded with 15ug of protein from the plasma exosome enriched pellets of their respective samples. AP, BP and CP represent lanes loaded with 15ug of protein extracted from plasma of the same subject. This gel stain demonstrates that the content of the pellets is similar both between subjects, and between the pellets obtained from different samples from the same subject.

further supported by Figure 8, which is a Western blot probing for CD81, which is a tetraspanin that is a known marker of exosomes. The blot compares the 200,000xg pellets of samples B, C1, C2, and C3 to the supernatant from that spin. Sample A was omitted because the presence of CD81 in the pellet obtained from this subject's plasma had already been validated. This blot

Figure 8

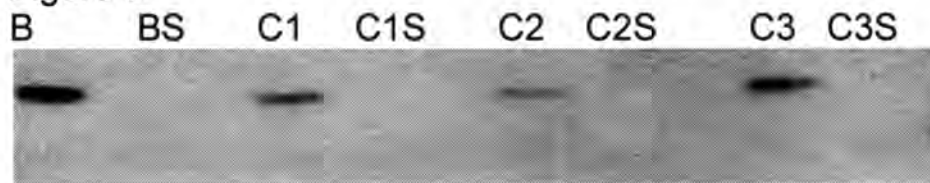


Fig 8 is a Western blot probing for CD81, a known exosome marker. Lanes contain 15ug of protein obtained from the 200,000xg pellet (e.g. C1) or the supernatant from that spin (e.g. C1S). This blot demonstrates that CD81 is present in the pellets, but not the supernatant.

demonstrates that CD81 is present in the pellets, but not in the supernatant, which indicates that the pellet is enriched in exosomes. Again, this is shown both from subject to subject and in the pellets obtained from the triplicate samples from subject C.

In summary, there was considerable variability in the total amount of protein obtained from the exosome-enriched pellets of the three subjects. This indicates that there is biological variability in the amount of protein that is present in the exosome-enriched pellets. Comparison of the 1D gel profiles of the pellets from subjects A, B, and C demonstrates that the content of the pellets is similar from person to person, although there are some differences in the banding patterns, specifically around 60kD and less than 25kD. The relative enrichment of CD81 seen in the pellet from subjects B and C by Western blot analysis is further evidence of the similarity of their contents. Specifically, this demonstrates that exosomes were enriched in each of the pellets. Taken together, these data indicate that while different amounts of protein are obtained from the exosome-enriched pellets of different subjects, the pellets contain similar, but not identical, proteomes. Importantly, there was a much smaller degree of variability in the 3 pellets isolated from the plasma samples of subject C. Approximately 15%

variation was observed in the total amount of protein obtained. Additionally, while sample C3 had a small shift in the band located at 60kD, the 1D gel banding patterns appear to be comparable in these 3 samples. In summary, there is little variability in the amount of protein contained in the pellets from the three samples from subject C. Additionally, the pellets appear to be comparable in content, as demonstrated by 1D gel electrophoresis. Similarly, Western blot analysis found that all three pellets were enriched in CD81 compared to the supernatant from the 200,000xg spin. These data suggest that the degree of technical variability in our protocol is acceptable. In conclusion, the results of this study indicate that the protocol yields a pellet that is similar in content from person to person, and it reproducibly yields comparable amounts of protein from the plasma exosome-enriched pellet, when biological variability is controlled. These data indicate that the protocol is a reliable means to obtain a plasma exosome-enriched pellet, which can be analyzed with proteomics methods in order to identify potential biomarkers.

III. Acute GVHD Biomarker Discovery Study

The culmination of our study was a biomarker discovery project for acute Graft-Versus-Host disease (acute GVHD). We used 7 banked plasma samples that had been obtained on day 7 after allogeneic hematopoietic stem cell transplantation. Three patients developed severe acute GVHD after this time, and 4 did not. The protein content of exosome enriched pellets of these patients were analyzed by matrix-assisted laser desorption ionization tandem mass spectrometry (MALDI MS/MS). Thirty-seven proteins were identified with 66% confidence and a 1% false discovery rate. The proteins identified are listed in Table 5.

Our goal was to discover predictive biomarkers of acute GVHD using proteomic analysis of plasma exosomes. Exosomes are a logical choice for biomarker discovery projects, because they contain cell-specific components, and can therefore allow us to understand what is occurring on a cellular level. However, exosomes are not very abundant in plasma. In order to study them, they must be concentrated, and the high abundance proteins present in plasma must be depleted. This is because the high abundance proteins tend to overshadow lower abundance proteins during proteomic analysis. This is undesirable because the lower abundance proteins are much more numerous than the higher abundance ones, and therefore we are much more likely to identify a biomarker by analyzing them. Unfortunately, many of the proteins that we identified were high abundance plasma proteins. While this is a limitation of our data, it must be noted that we cannot exclude the possible association of

Table 5. Proteins Identified in the Plasma Exosome-Enriched Pellets of Allo-HSCT Patients

Proteins Identified By Multiple Peptides	Proteins Identified By a Single Peptide	Proteins Identified By Peptide Mass Fingerprinting
1) alpha-2-macroglobulin 2) Ig mu chain C region 3) Fibrinogen alpha chain 4) Fibrinogen beta chain 5) Complement C3 6) Ig kappa chain C region 7) Serum albumin 8) Ig lambda chain C region 9) Fibronectin 10) Ig gamma-3 chain C region 11) von Willebrand factor 12) Complement C4-B 13) Complement C4-A 14) C4b-binding protein alpha chain 15) Ig alpha-1 chain C region 16) Ig alpha-2 chain C region 17) Fibrinogen gamma chain 18) Ig mu heavy chain disease protein 18) Ig heavy chain V-III region TEI 19) Ig heavy chain V-III region BRO	1) Ig heavy chain V-III region VH26 2) Ig heavy chain V-III region WAS 3) Ig heavy chain V-III region POM 4) Ig heavy chain V-III region TUR 5) Ig heavy chain V-III region TIL 6) ferritin light chain 7) Ig heavy chain V-III region TEI 8) Ig heavy chain V-III region BRO 9) Dedicator of cytokinesis protein 1 10) Histidine-rich glycoprotein 11) Immunoglobulin J chain 12) Ig kappa chain V-I region AU 13) Ig kappa chain V-I region GAL 14) Ig kappa chain V-I region HAU 15) Ig kappa chain V-I region DAUDI 16) Ig kappa chain V-I region WALKER 17) Ig kappa chain V-I region Roy 18) Ig kappa chain V-I region WAT 19) Ig kappa chain V-I region Rei 20) Ig kappa chain V-I region WEA 21) Ig kappa chain V-I region Scw 22) Ig kappa chain V-I region HK101 23) Ig kappa chain V-I region AG	1) DENN domain-containing protein 4B 2) Abnormal spindle-like microencephaly-associated protein 3) Ig heavy chain V-I region V35 4) Collagen alpha-1 (XV) 5) Growth factor receptor-bound protein 10 6) Lysine-specific demethylase 2B 7) EF-hand calcium-binding domain-containing protein 2 8) Sulfate transporter 9) Transmembrane protease, serine 13

these proteins with plasma exosomes. Indeed, as was mentioned in the literature review, B lymphocyte derived exosomes are known to harbor immunoglobulins, which comprised a large percentage of the proteins that we identified. Alternatively, the presence of these high abundance proteins in the exosome-enriched pellet could be because these proteins adhere to plasma exosomes, or because the speed at which we centrifuged the plasma to isolate exosomes (200,000xg) was great enough to pull these proteins down as well.

Perhaps in the future, it would be advisable to treat our samples with a reducing agent such as dithiothreitol to remove any proteins that may be adherent to the surface of the exosomes. Similarly, centrifuging the plasma at lower speeds may reduce the amount of high abundance protein that is pulled down in the exosome-enriched pellet. Having said all that, the presence of the higher abundance plasma proteins in the pellets does not exclude the presence of exosomes in it. While we have no way of knowing for sure with these particular samples, given our previous electron micrographs and Western blot data, we are confident that exosomes were present in the pellet. In all likelihood the proteins in the exosomes that were pulled down during ultracentrifugation were overshadowed by the higher abundance proteins, which were also pelleted. Therefore, if this protocol is to be used in the future, steps need to be taken to purify the pelleted exosomes from the high abundance proteins which are also in the pellet. This could be done using a sucrose density gradient or similar gradient.

Since we were looking for biomarkers of acute GVHD, we were not only interested in the proteins that we could identify, but also in their relative quantities between cases and controls. Therefore, the samples were labeled with the isobaric tag iTRAQ prior to MS/MS analysis. By calculating the intensity of each of the seven iTRAQ labels for each peptide/protein that we identified, we were able to determine their relative quantities in each sample. The data generated from this experiment was further analyzed using iQuantitator, an in-house statistical software program designed by John Schwacke, PhD. This analysis

grouped the samples into acute GVHD cases and controls and compared the relative abundance of sequenced peptides and proteins between the two groups. The summary figure of this analysis is presented in Figure 9. The dots represent the median relative abundance in acute GVHD cases. A value of 0.5 would indicate that the median value for the acute GVHD patients is half that of controls, and a value of 2 is indicative of the median value for acute GVHD patients being twice that of controls. A value of 1 indicates that the medians for the acute GVHD patients is the same as that of controls. The lines extending from the dot represent credible intervals. The significance of a credible interval is analogous to that of a confidence interval. In other words, only those proteins whose credible intervals do not span 1 are really different in abundance between the two groups.

Notably, the credible intervals for all of the identified proteins are quite large, and none of the identified proteins had a credible interval that did not cross 1 (see Figure 9). Therefore, using this method, we were not able to identify any proteins that were definitely differentially abundant between those patients who developed acute GVHD and those who did not. It appears that width of the credible intervals is the major cause of our inability to discriminate between the two groups. This could be due to the large amount of noise present in the MS/MS spectra for our samples, which may be the result of the parameters used during MALDI TOF-TOF MS/MS analysis. Despite the fact that this analysis failed to yield a biomarker that can definitively discriminate between cases and

controls, the data do yield some interesting clues as to what immunologic events may be occurring in these patients.

Of particular importance are the credible intervals for Ig lambda C region and the Ig kappa C region (see Figure 10 for iQuantitator output of the individual peptides of kappa and lambda). These two proteins make up the constant region of the immunoglobulin light chains lambda and kappa, respectively. The credible interval of Ig lambda C region is 0.88-2.1, and the median value is 1.35. This indicates that the median amount of Ig lambda C region is 35% greater in cases compared to controls, but based on this data the true median could be from 88% to 210% of controls. In contrast, the credible interval of Ig kappa C region is 0.59, 1.21 and median value is 0.85, meaning that the median amount of Ig kappa C region in cases is 85% that of controls. However, the true median could lie between 59% and 121% of controls. Because these credible intervals include 1, the data do not prove that cases and controls have different amounts of kappa and lambda light chains. However, the data are still significant because there is a known relationship in the ratio of kappa and lambda light chains. In order to understand the significance, it is first necessary to briefly review immunoglobulin structure.

Immunoglobulins are composed of two heavy chains and two light chains. Heavy chains and light chains each have a variable region and a constant region. The constant regions are antigenically different, and are the basis for the classification of immunoglobulins. The constant region of the heavy chain determines to which class the antibody belongs. A given heavy chain can have

Figure 9a Relative Quantities of Proteins Identified by More Than One Peptide

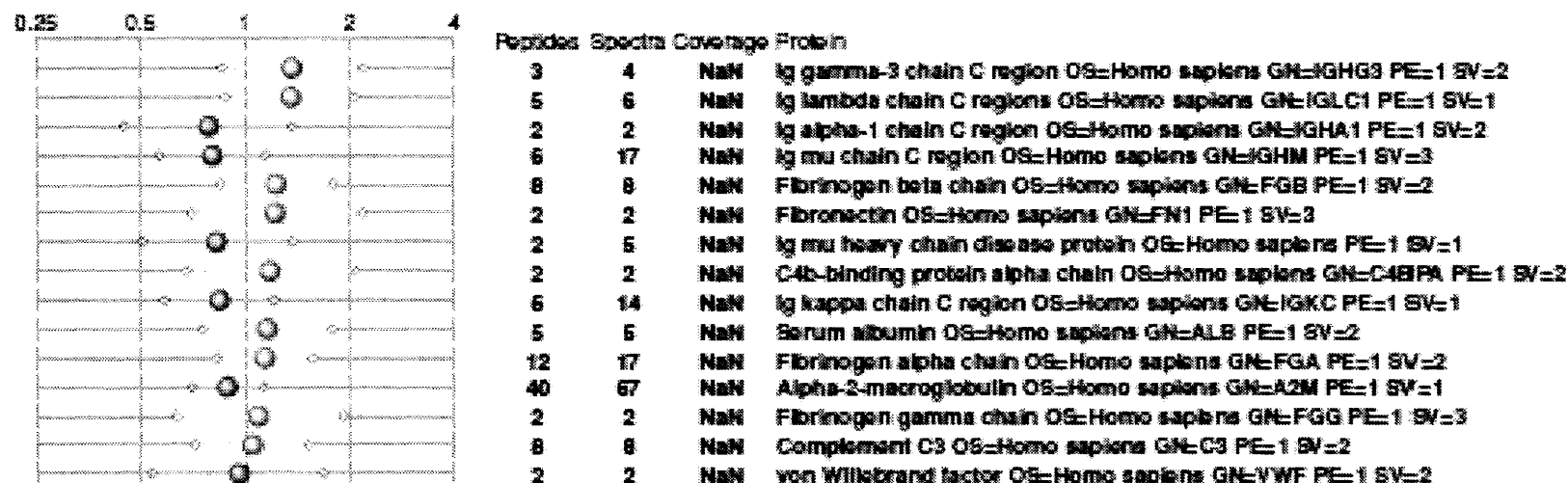


Figure 9b Relative Quantities of Proteins Identified by a Single Peptide

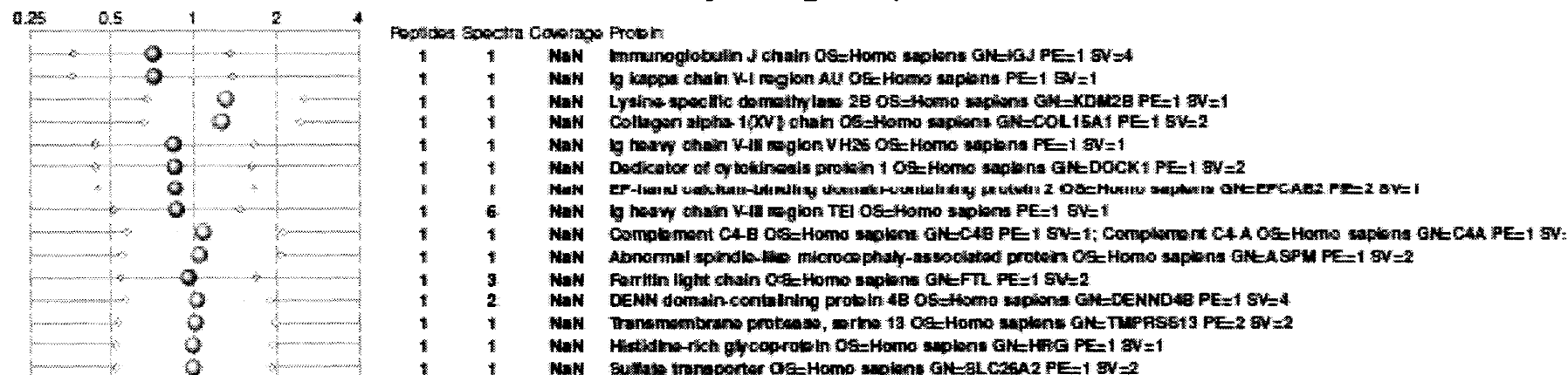


Figure 9 is the visual output of iQuantitor iTRAQ analysis for identified proteins. Values greater than 1 indicate higher abundance in cases. Values less than one indicate lower abundance in cases, whereas values greater than 1 indicate higher abundance in cases.

Figure 10a Relative Quantities of Lambda C Region Peptides

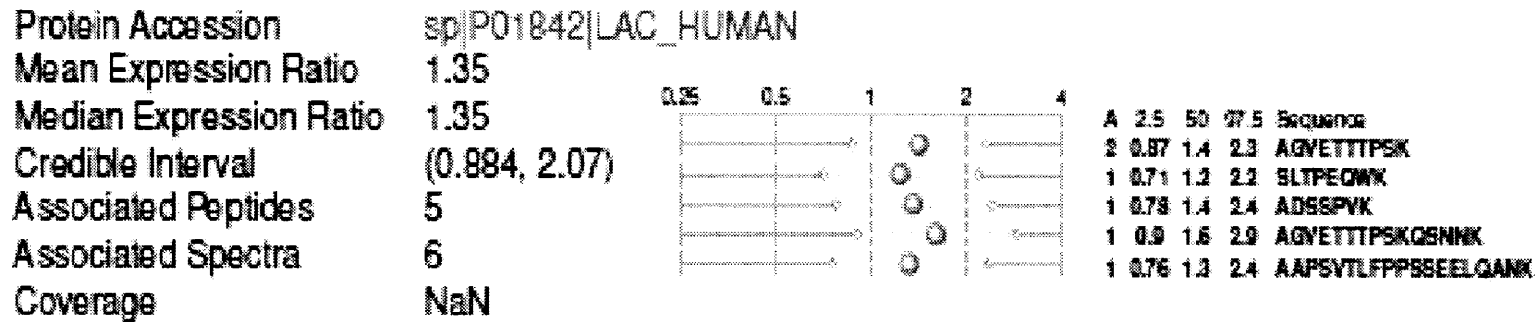


Figure 10b Relative Quantities of Kappa C Region Peptides

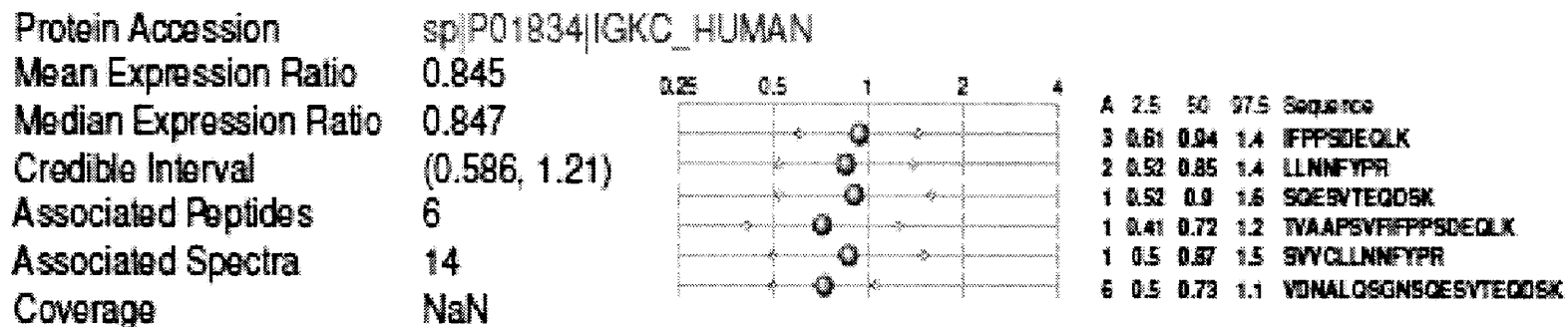


Figure 10 is the visual output of iQuantitator iTRAQ analysis for the identified peptides of lambda and kappa light chains. Values greater than 1 indicate higher abundance in cases. Values less than one indicate lower abundance in cases, whereas values greater than 1 indicate higher abundance in cases.

one of five isotypes: alpha, gamma, mu, delta, and epsilon. Consequently there are five classes of antibody: alpha (IgA), gamma (IgG), mu (IgM), delta (IgD), and epsilon (IgE). Additionally, there are two isotypes of immunoglobulin light chains: kappa and lambda. Therefore, each antibody is comprised of a single isotype of heavy chain (e.g. gamma), and a single isotype of light chain (e.g. kappa), although it has two of each chain. The reasons that each antibody is restricted to having one isotype of heavy chain and one isotype of light chain are complicated and beyond the scope of this discussion. Suffice it to say that complex genetic rearrangements that occur during B cell development result in the exclusion of all of the alleles of the heavy chain and light chain genes except for one of each, which are used to produce a functional antibody. While it is true that B cells can switch the class of antibody that they produce by rearranging the genes for the heavy chain constant region, this does not occur in with light chains. Therefore, once a B cell begins to make antibodies with a given light chain isotype, that isotype does not change.

Another salient point is that B cells (and plasma cells) produce excess light chains during antibody production. The excess light chains are secreted, and may be found in bodily fluids such as plasma and urine.[70,71] These are called free light chains. Ordinarily, there are approximately twice as many B cells and plasma cells that make antibodies containing kappa light chain compared to lambda light chain. Thus the mean total kappa:lambda in plasma is 1.78 in normal patients.[72] Total kappa:lambda includes all of the light chains that are bound up in antibodies, and the free light chains present in plasma. Because of

Formula 1

$$\frac{R_D}{R_C} = \frac{P_{\kappa,D} P_{\lambda,C}}{P_{\lambda,D} P_{\kappa,C}}$$

Formula 1 was used to calculate the ratio of treatment effects for kappa:lambda. R_D is the kappa:lambda ratio in patients who developed acute GVHD, whereas R_C is the kappa:lambda ratio of patients who did not develop acute GVHD. P_{κ} and P_{λ} are the abundances of kappa and lambda respectively.

differences in the rates of plasma clearance of the free light chains, the free kappa: free lambda ratio is approximately 0.6.[72] The interest in these ratios is that any aberration thereof is an indicator of monoclonal expansion, since B cells and plasma cells can only make one of the two light chain isotypes. Thus they are often used in the diagnosis of plasma cell dyscrasias such as multiple myeloma.

Knowing this sheds new light on the data from our iTRAQ study. Even though the credible intervals of the constant regions of lambda light chain and kappa light chain cross 1, it is intriguing to note that the median value for the constant region of lambda light chain is up in cases, whereas the median value for both the constant region and a variable region of kappa light chain is down in cases. Furthermore, the majority of the distribution of the credible intervals lies on one side of 1. Given the inverse relationship between kappa and lambda levels, this would appear to be consistent with a monoclonal expansion, although we cannot be certain given this data. To test the hypothesis that the kappa:lambda ratio of the plasma exosome-enriched pellets was different in cases compared to controls, we took an *a posteriori* statistical approach.

Figure 11

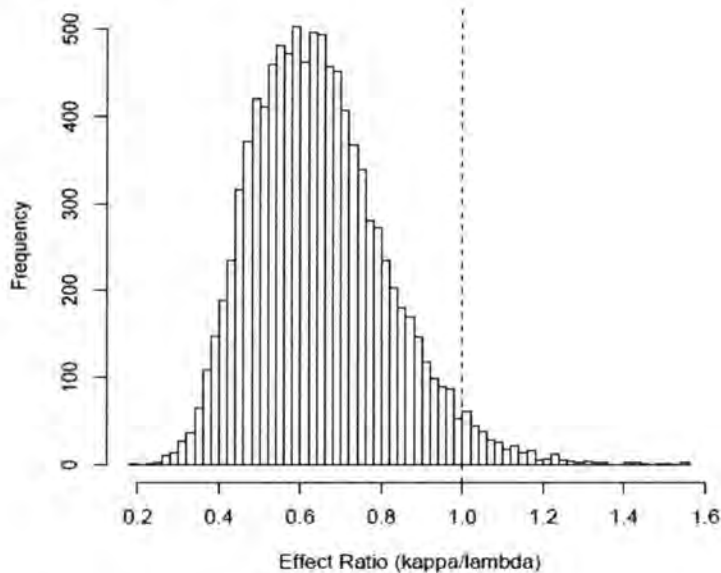


Figure 11 is the posterior distribution of R_D/R_C . A value of 1 would indicate that the two groups have equal kappa:lambda ratios.

would indicate that the two groups are no different. The calculated value from our data was 0.63, with a 95% CI of 0.38, 1.03. Using a Bayesian modeling approach, we generated a histogram of the posterior distribution of this estimate, which is shown in Figure 11. To determine the probability of observing such a distribution in our data, we used the same approach to generate a null distribution from our data. Briefly, we bootstrap sampled 5,000 pairs of proteins, and calculated the ratio of treatment effects and effective z scores for each pair. Comparing the kappa:lambda ratio of treatment effects to this null distribution, we calculated a p-value of 0.011. Therefore, our data seem to indicate that the day 7 posttransplantation kappa:lambda ratio differs between patients who later develop severe acute GVHD and those who do not.

We used the iQuantitator output data from our iTRAQ experiment to calculate a ratio of treatment effects. This was done by dividing the case kappa:lambda ratio by the control kappa:lambda ratio (see Formula 1 for the equation). A value of 1

Also of importance are the results for the IgG3 constant region. Its credible interval is 1.86 to 2.2 and its median is 1.36 (see Figure 8 for iQuantitator output for individual peptides of IgG3 constant region). While this is not statistically significant, data from a classification tree generated by random forest suggests that relative IgG3 levels may be an important distinguishing characteristic between cases and controls. Random forest uses a subset of the data to generate a series of classification trees. Each classification tree is then tested for its accuracy using the rest of the data. The best classification tree that was generated was able to distinguish between cases and controls with 70% accuracy. In this classification tree, the variable with the most weight (i.e. the greatest ability to distinguish between cases and controls) was IgG3. The importance of potential differences in plasma IgG3 levels between acute GVHD cases and controls is apparent given its unique properties. IgG3 is one of four subclasses of IgG, which are distinguished from one another by their antigenically unique constant regions. The most prevalent subclass of IgG in plasma is IgG1, and IgG3 usually only makes up a small percentage of total IgG. And increased amounts of IgG3 have been associated with autoimmunity. While the reasons for this association are not entirely understood, it is plausible that this is due to its unique structure. The constant region of IgG3 has a longer hinge region than other IgG subclasses. This increases its effectiveness at fixing and activating complement. Additionally, the constant region of IgG3 has greater affinity for the Fc-gamma I receptor than other IgG subclasses. Therefore it is the most effective at initiating antibody-dependent cellular cytotoxicity and

opsonization. Together, these qualities suggest that higher levels of circulating IgG3 could result in the increased tissue damage that is seen in autoimmunity. Since there is some overlap in the pathophysiology of acute GVHD and autoimmunity, it seems reasonable that there could be a link between IgG3 levels in plasma and the onset of acute GVHD. It is also important to note that the half-life of IgG3 is considerably shorter than other IgG subtypes. For example, the half-life of plasma IgG1 is 21 days, whereas IgG3 has a half-life of 6-7 days. Our samples were obtained on day 7 posttransplantation. Since approximately 1 week is required for the generation of a primary humoral response, which is mostly composed of IgM, it is unlikely that any increase in IgG3 after transplantation is a result of donor B cells reacting against alloantigens. Furthermore, allogeneic hematopoietic stem cell transplantation is often associated with dysfunction in humoral immunity, especially early after transplantation. This makes it even more unlikely that increased IgG3 on day 7 posttransplantation would be the result of an anti-donor humoral response. Having said that, it seems more plausible that patients with higher levels of circulating IgG3 at the time of transplantation are at increased risk of developing acute GVHD later on. This could be due to increased complement fixation and activation, which would result in increased tissue damage and subsequent presentation of alloantigens. With this data, however, we cannot necessarily make this claim.

Conclusion and Future Directions

Discovery driven proteomics is a powerful research tool. Its primary use is the unbiased generation of data that can lead to the formulation of testable hypotheses. In fact, that was the purpose of this project, to discover potential early biomarkers of acute Graft-Versus-Host disease (GVHD) that could be validated in later work. The results of our study indicate that markers of B cell activation and proliferation might be useful diagnostic tools early after allogeneic hematopoietic stem cell transplantation. They are part of a growing body of evidence that suggests a role for B cells in the pathogenesis of acute GVHD. Specifically, it has been demonstrated that refractory acute GVHD may respond to rituximab therapy (rituximab is an anti-CD20 monoclonal antibody that targets B cells).[73] Additionally, administration of rituximab during the pretransplantation conditioning regimen or soon after transplantation has been shown to decrease the incidence of acute GVHD.[74-76] In light of our results and the published results of other studies, we hypothesize that analysis of kappa:lambda ratios early after allogeneic hematopoietic stem cell transplantation can be used to predict later diagnosis of severe acute GVHD. In order to test this hypothesis, we propose the following validation study. We will obtain blood samples on posttransplantation days 0, 7, and 21 from patients who have undergone allogeneic hematopoietic stem cell transplantation. We will also obtain sample at the time of acute GVHD diagnosis. From these samples, we will

quantify kappa and lambda light chains using the protocol that has been presented in here. This will allow us to validate the clinical utility of using kappa:lambda light chain ratios of the plasma exosome-enriched pellet to predict the occurrence of severe acute GVHD. We also propose to analyze these same samples with commercially available serum light chain test in order to determine if similar results can be obtained using these tests. Finally, we will use the samples obtained at the time of diagnosis to determine if kappa:lambda ratios remain aberrant during later stages of the disease. Data from these tests will be used to determine if kappa:lambda ratios are predictive of the development of acute GVHD.

Bibliography

1. Copelan, E.A., *Hematopoietic stem-cell transplantation*. N Engl J Med, 2006. **354**(17): p. 1813-26.
2. Ferrara, J.L., et al., *Graft-versus-host disease*. Lancet, 2009. **373**(9674): p. 1550-61.
3. Goulmy, E., et al., *Mismatches of minor histocompatibility antigens between HLA-identical donors and recipients and the development of graft-versus-host disease after bone marrow transplantation*. N Engl J Med, 1996. **334**(5): p. 281-5.
4. Rowlings, P.A., et al., *IBMTR Severity Index for grading acute graft-versus-host disease: retrospective comparison with Glucksberg grade*. Br J Haematol, 1997. **97**(4): p. 855-64.
5. MacMillan, M.L., et al., *Response of 443 patients to steroids as primary therapy for acute graft-versus-host disease: comparison of grading systems*. Biol Blood Marrow Transplant, 2002. **8**(7): p. 387-94.
6. Cragg, L., et al., *A randomized trial comparing prednisone with antithymocyte globulin/prednisone as an initial systemic therapy for moderately severe acute graft-versus-host disease*. Biol Blood Marrow Transplant, 2000. **6**(4A): p. 441-7.
7. Cahn, J.Y., et al., *Prospective evaluation of 2 acute graft-versus-host (GVHD) grading systems: a joint Societe Francaise de Greffe de Moelle et Therapie Cellulaire (SFGM-TC), Dana Farber Cancer Institute (DFCI), and International Bone Marrow Transplant Registry (IBMTR) prospective study*. Blood, 2005. **106**(4): p. 1495-500.
8. Reits, E.A., et al., *Radiation modulates the peptide repertoire, enhances MHC class I expression, and induces successful antitumor immunotherapy*. J Exp Med, 2006. **203**(5): p. 1259-71.
9. Matte, C.C., et al., *Donor APCs are required for maximal GVHD but not for GVL*. Nat Med, 2004. **10**(9): p. 987-92.
10. Reddy, P., et al., *A crucial role for antigen-presenting cells and alloantigen expression in graft-versus-leukemia responses*. Nat Med, 2005. **11**(11): p. 1244-9.
11. Nikolic, B., et al., *Th1 and Th2 mediate acute graft-versus-host disease, each with distinct end-organ targets*. J Clin Invest, 2000. **105**(9): p. 1289-98.
12. Wysocki, C.A., et al., *Leukocyte migration and graft-versus-host disease*. Blood, 2005. **105**(11): p. 4191-9.

13. Welniak, L.A., B.R. Blazar, and W.J. Murphy, *Immunobiology of allogeneic hematopoietic stem cell transplantation*. *Annu Rev Immunol*, 2007. **25**: p. 139-70.
14. Paczesny, S., et al., *A biomarker panel for acute graft-versus-host disease*. *Blood*, 2009. **113**(2): p. 273-8.
15. Weissinger, E.M., et al., *Proteomic patterns predict acute graft-versus-host disease after allogeneic hematopoietic stem cell transplantation*. *Blood*, 2007. **109**(12): p. 5511-9.
16. Srinivasan, R., et al., *Accurate diagnosis of acute graft-versus-host disease using serum proteomic pattern analysis*. *Exp Hematol*, 2006. **34**(6): p. 796-801.
17. Paczesny, S., et al., *Elafin is a biomarker of graft-versus-host disease of the skin*. *Sci Transl Med*. **2**(13): p. 13ra2.
18. Wolf, P., *The nature and significance of platelet products in human plasma*. *Br J Haematol*, 1967. **13**(3): p. 269-88.
19. Pan, B.T., R. Blostein, and R.M. Johnstone, *Loss of the transferrin receptor during the maturation of sheep reticulocytes in vitro. An immunological approach*. *Biochem J*, 1983. **210**(1): p. 37-47.
20. Pan, B.T. and R.M. Johnstone, *Fate of the transferrin receptor during maturation of sheep reticulocytes in vitro: selective externalization of the receptor*. *Cell*, 1983. **33**(3): p. 967-78.
21. Pan, B.T. and R. Johnstone, *Selective externalization of the transferrin receptor by sheep reticulocytes in vitro. Response to ligands and inhibitors of endocytosis*. *J Biol Chem*, 1984. **259**(15): p. 9776-82.
22. Pan, B.T., et al., *Electron microscopic evidence for externalization of the transferrin receptor in vesicular form in sheep reticulocytes*. *J Cell Biol*, 1985. **101**(3): p. 942-8.
23. Johnstone, R.M., M. Adam, and B.T. Pan, *The fate of the transferrin receptor during maturation of sheep reticulocytes in vitro*. *Can J Biochem Cell Biol*, 1984. **62**(11): p. 1246-54.
24. Johnstone, R.M., *Revisiting the road to the discovery of exosomes*. *Blood Cells Mol Dis*, 2005. **34**(3): p. 214-9.
25. Fevrier, B. and G. Raposo, *Exosomes: endosomal-derived vesicles shipping extracellular messages*. *Curr Opin Cell Biol*, 2004. **16**(4): p. 415-21.
26. Wollert, T., et al., *Membrane scission by the ESCRT-III complex*. *Nature*, 2009. **458**(7235): p. 172-7.

27. Wollert, T. and J.H. Hurley, *Molecular mechanism of multivesicular body biogenesis by ESCRT complexes*. *Nature*. **464**(7290): p. 864-9.
28. Geminard, C., et al., *Degradation of AP2 during reticulocyte maturation enhances binding of hsc70 and Alix to a common site on TFR for sorting into exosomes*. *Traffic*, 2004. **5**(3): p. 181-93.
29. de Gassart, A., et al., *Lipid raft-associated protein sorting in exosomes*. *Blood*, 2003. **102**(13): p. 4336-44.
30. Thery, C., M. Ostrowski, and E. Segura, *Membrane vesicles as conveyors of immune responses*. *Nat Rev Immunol*, 2009. **9**(8): p. 581-93.
31. Peters, P.J., et al., *Molecules relevant for T cell-target cell interaction are present in cytolytic granules of human T lymphocytes*. *Eur J Immunol*, 1989. **19**(8): p. 1469-75.
32. Peters, P.J., et al., *A new model for lethal hit delivery by cytotoxic T lymphocytes*. *Immunol Today*, 1990. **11**(1): p. 28-32.
33. Peters, P.J., et al., *Cytotoxic T lymphocyte granules are secretory lysosomes, containing both perforin and granzymes*. *J Exp Med*, 1991. **173**(5): p. 1099-109.
34. Mathivanan, S. and R.J. Simpson, *ExoCarta: A compendium of exosomal proteins and RNA*. *Proteomics*, 2009. **9**(21): p. 4997-5000.
35. Blanchard, N., et al., *TCR activation of human T cells induces the production of exosomes bearing the TCR/CD3/zeta complex*. *J Immunol*, 2002. **168**(7): p. 3235-41.
36. Muntasell, A., A.C. Berger, and P.A. Roche, *T cell-induced secretion of MHC class II-peptide complexes on B cell exosomes*. *EMBO J*, 2007. **26**(19): p. 4263-72.
37. Saunderson, S.C., et al., *Induction of exosome release in primary B cells stimulated via CD40 and the IL-4 receptor*. *J Immunol*, 2008. **180**(12): p. 8146-52.
38. Raposo, G., et al., *B lymphocytes secrete antigen-presenting vesicles*. *J Exp Med*, 1996. **183**(3): p. 1161-72.
39. Denzer, K., et al., *Follicular dendritic cells carry MHC class II-expressing microvesicles at their surface*. *J Immunol*, 2000. **165**(3): p. 1259-65.
40. Beauvillain, C., et al., *A vaccine based on exosomes secreted by a dendritic cell line confers protection against *T. gondii* infection in syngeneic and allogeneic mice*. *Microbes Infect*, 2007. **9**(14-15): p. 1614-22.
41. Beauvillain, C., et al., *Exosomes are an effective vaccine against congenital toxoplasmosis in mice*. *Vaccine*, 2009. **27**(11): p. 1750-7.
42. Zitvogel, L., et al., *Eradication of established murine tumors using a novel cell-free vaccine: dendritic cell-derived exosomes*. *Nat Med*, 1998. **4**(5): p. 594-600.

43. They, C., et al., *Indirect activation of naive CD4+ T cells by dendritic cell-derived exosomes*. Nat Immunol, 2002. **3**(12): p. 1156-62.
44. Andre, F., et al., *Exosomes as potent cell-free peptide-based vaccine. I. Dendritic cell-derived exosomes transfer functional MHC class I/peptide complexes to dendritic cells*. J Immunol, 2004. **172**(4): p. 2126-36.
45. Segura, E., et al., *ICAM-1 on exosomes from mature dendritic cells is critical for efficient naive T-cell priming*. Blood, 2005. **106**(1): p. 216-23.
46. Segura, E., et al., *CD8+ dendritic cells use LFA-1 to capture MHC-peptide complexes from exosomes in vivo*. J Immunol, 2007. **179**(3): p. 1489-96.
47. Nolte-'t Hoen, E.N., et al., *Activated T cells recruit exosomes secreted by dendritic cells via LFA-1*. Blood, 2009. **113**(9): p. 1977-81.
48. Hao, S., et al., *Mature dendritic cells pulsed with exosomes stimulate efficient cytotoxic T-lymphocyte responses and antitumour immunity*. Immunology, 2007. **120**(1): p. 90-102.
49. Admyre, C., et al., *Direct exosome stimulation of peripheral human T cells detected by ELISPOT*. Eur J Immunol, 2006. **36**(7): p. 1772-81.
50. Helft, J., et al., *Antigen-specific T-T interactions regulate CD4 T-cell expansion*. Blood, 2008. **112**(4): p. 1249-58.
51. Escudier, B., et al., *Vaccination of metastatic melanoma patients with autologous dendritic cell (DC) derived-exosomes: results of the first phase I clinical trial*. J Transl Med, 2005. **3**(1): p. 10.
52. Morse, M.A., et al., *A phase I study of dexosome immunotherapy in patients with advanced non-small cell lung cancer*. J Transl Med, 2005. **3**(1): p. 9.
53. Viaud, S., et al., *Dendritic cell-derived exosomes promote natural killer cell activation and proliferation: a role for NKG2D ligands and IL-15Ralpha*. PLoS One, 2009. **4**(3): p. e4942.
54. Simhadri, V.R., et al., *Dendritic cells release HLA-B-associated transcript-3 positive exosomes to regulate natural killer function*. PLoS One, 2008. **3**(10): p. e3377.
55. Peche, H., et al., *Presentation of donor major histocompatibility complex antigens by bone marrow dendritic cell-derived exosomes modulates allograft rejection*. Transplantation, 2003. **76**(10): p. 1503-10.
56. Peche, H., et al., *Induction of tolerance by exosomes and short-term immunosuppression in a fully MHC-mismatched rat cardiac allograft model*. Am J Transplant, 2006. **6**(7): p. 1541-50.

57. Chaput, N., et al., *Exosomes as potent cell-free peptide-based vaccine. II. Exosomes in CpG adjuvants efficiently prime naive Tc1 lymphocytes leading to tumor rejection.* J Immunol, 2004. **172**(4): p. 2137-46.
58. Guo, F., et al., *Anti-tumour effects of exosomes in combination with cyclophosphamide and polyinosinic-polycytidylic acid.* J Int Med Res, 2008. **36**(6): p. 1342-53.
59. Lutsiak, M.E., et al., *Inhibition of CD4(+)25+ T regulatory cell function implicated in enhanced immune response by low-dose cyclophosphamide.* Blood, 2005. **105**(7): p. 2862-8.
60. Taieb, J., et al., *Chemoimmunotherapy of tumors: cyclophosphamide synergizes with exosome based vaccines.* J Immunol, 2006. **176**(5): p. 2722-9.
61. Miranda, K.C., et al., *Nucleic acids within urinary exosomes/microvesicles are potential biomarkers for renal disease.* Kidney Int. **78** (2): p. 191-9.
62. Hunter, M.P., et al., *Detection of microRNA expression in human peripheral blood microvesicles.* PLoS One, 2008. **3**(11): p. e3694.
63. Taylor, D.D. and C. Gercel-Taylor, *MicroRNA signatures of tumor-derived exosomes as diagnostic biomarkers of ovarian cancer.* Gynecol Oncol, 2008. **110**(1): p. 13-21.
64. Zhou, H., et al., *Urinary exosomal transcription factors, a new class of biomarkers for renal disease.* Kidney Int, 2008. **74**(5): p. 613-21.
65. Michael, A., et al., *Exosomes from human saliva as a source of microRNA biomarkers.* Oral Dis. **16**(1): p. 34-8.
66. Rabinowits, G., et al., *Exosomal microRNA: a diagnostic marker for lung cancer.* Clin Lung Cancer, 2009. **10**(1): p. 42-6.
67. Logozzi, M., et al., *High levels of exosomes expressing CD63 and caveolin-1 in plasma of melanoma patients.* PLoS One, 2009. **4**(4): p. e5219.
68. Li, J., et al., *Claudin-containing exosomes in the peripheral circulation of women with ovarian cancer.* BMC Cancer, 2009. **9**: p. 244.
69. Pisitkun, T., R.F. Shen, and M.A. Knepper, *Identification and proteomic profiling of exosomes in human urine.* Proc Natl Acad Sci U S A, 2004. **101**(36): p. 13368-73.
70. Ambrosino, D.M., et al., *Human B cells secrete predominantly lambda L chains in the absence of H chain expression.* J Immunol, 1991. **146**(2): p. 599-602.
71. Mole, C.M., et al., *Light chains of immunoglobulins in human secretions.* Clin Chim Acta, 1994. **224**(2): p. 191-7.

72. Katzmann, J.A., et al., *Serum reference intervals and diagnostic ranges for free kappa and free lambda immunoglobulin light chains: relative sensitivity for detection of monoclonal light chains*. Clin Chem, 2002. **48**(9): p. 1437-44.

iTRAQ Data Analysis Report

Alge, Arthur Group

July 20, 2010

1 Introduction

This document summarizes an analysis of relative protein expression using iTRAQ. The reporter ion peak area measurements supplied by the ABI software are used to estimate treatment-dependent peptide and protein relative expression. Estimation is accomplished using a Bayesian approach with the model given below. The document includes a protein relative expression summary and a per-protein detailed analysis. The document is internally hyperlinked and linked externally to NCBI.

2 Experiment and Model Description

2.1 Experiment Design

The report summarizes data from one or more iTRAQ experiments addressing a common comparison. The experiment design, used in this analysis, is given in the table below.

	Experiment	Treatment	Channel	Sample
1	A	Control	113	S1
2	A	Case	114	S2
3	A	Case	115	S3
4	A	Control	116	S4
5	A	Control	117	S5
6	A	Control	118	S6
7	A	Case	119	S7

2.2 Input Files

Data for this analysis was extracted from the following tandem mass spectra (MSMS) summary files.

Experiment	MSMS Summary File
A	07.06.10_MUSC.csv

2.3 Statistical Model

The following statistical model was used to estimate the treatment-dependent effects.

$\text{LogIntensity} \sim \text{Channel} + \text{Spectrum} + \text{Protein} + \text{Peptide} + \text{Protein:Treatment} + \text{Peptide:Treatment}$

3 Data Summary

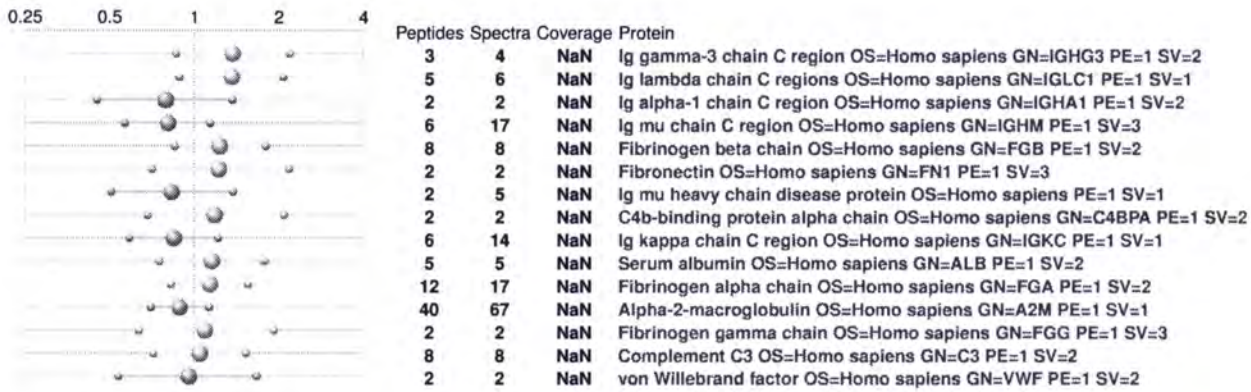
The data supplied in the MSMS summary is filtered to remove unidentified proteins, contaminants, and peptides containing selected modifications. The following table summarizes the data provided and used in the analysis.

	A	Combined
Supplied Spectra	1106	1106
Unidentified Spectra	857	857
Disallowed Modifications	2	2
Spectra from Contaminants	4	4
Missing Data	13	13
Low Confidence Spectra	857	857
Degenerate Peptides	46	46
Remaining Spectra		184
Unique Proteins		30
Unique Peptides		120
Model R^2		0.752

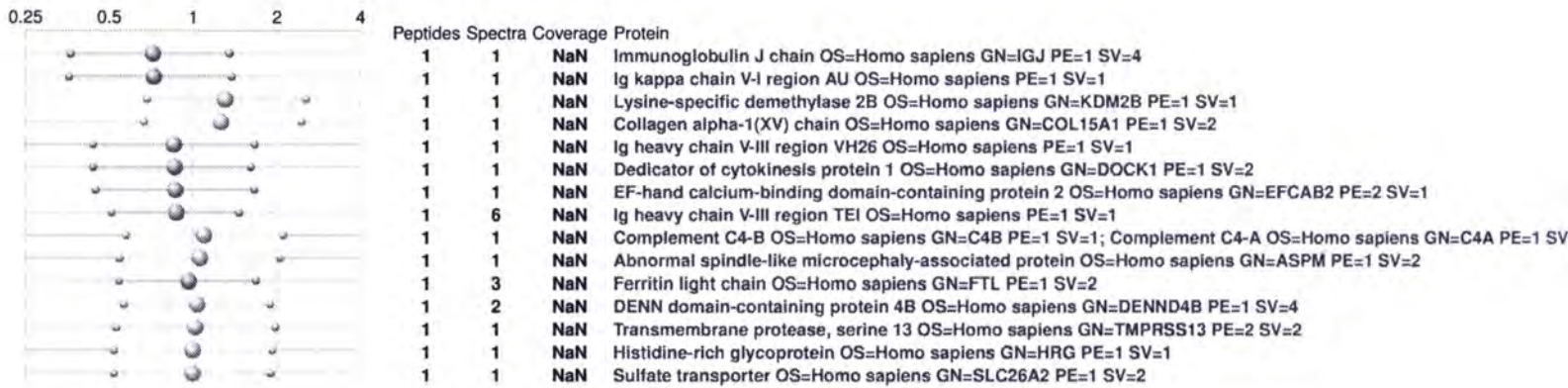
4 Protein Summary

Each protein identified in one or more of the MSMS summaries is listed below in decreasing order of expression change magnitude. The median and estimated credible interval for each protein is given to the left in the table. Proteins identified by a single peptide are listed in a separate table.

4.1 Identified Proteins



4.2 Proteins Identified by a Single Peptide



5 Protein Details

A detailed summary of each protein is given below. These sections include peptide relative expression estimates in addition to protein-level estimates.

5.1 Immunoglobulin J chain OS=Homo sapiens GN=IGJ PE=1 SV=4

Protein Accession	sp P01591 IGJ_HUMAN											
Mean Expression Ratio	0.713											
Median Expression Ratio	0.717											
Credible Interval	(0.362, 1.35)	0.25	0.5	1	2	4	A	2.5	50	97.5	Sequence	
Associated Peptides	1							1	0.31	0.61	1.2	SSEDPNEDIVER
Associated Spectra	1											
Coverage	NaN											

5.2 Ig kappa chain V-I region AU OS=Homo sapiens PE=1 SV=1

Protein Accession	sp P01594 KV102_HUMAN											
Mean Expression Ratio	0.717											
Median Expression Ratio	0.722											
Credible Interval	(0.358, 1.37)	0.25	0.5	1	2	4	A	2.5	50	97.5	Sequence	
Associated Peptides	1							1	0.30	0.62	1.2	DIQMTQSPSSLSASVGD
Associated Spectra	1											
Coverage	NaN											

5.3 Ig gamma-3 chain C region OS=Homo sapiens GN=IGHG3 PE=1 SV=2

Protein Accession	sp P01860 IGHG3_HUMAN											
Mean Expression Ratio	1.37											
Median Expression Ratio	1.36											
Credible Interval	(0.857, 2.19)	0.25	0.5	1	2	4	A	2.5	50	97.5	Sequence	
Associated Peptides	3							2	0.74	1.2	2.1	ALPAPIEK
Associated Spectra	4							1	0.94	1.7	3.1	EPQVYTLPPSREEMTK
Coverage	NaN							1	0.8	1.4	2.5	TLPPSREEMTK

5.4 Ig lambda chain C regions OS=Homo sapiens GN=IGLC1 PE=1 SV=1

Protein Accession	sp P01842 LAC_HUMAN											
Mean Expression Ratio	1.35											
Median Expression Ratio	1.35											
Credible Interval	(0.884, 2.07)	0.25	0.5	1	2	4	A	2.5	50	97.5	Sequence	
Associated Peptides	5							2	0.87	1.4	2.3	AGVETTTPSK
Associated Spectra	6							1	0.71	1.2	2.2	SLTPEQWK
Coverage	NaN							1	0.78	1.4	2.4	ADSSPVK
								1	0.9	1.6	2.9	AGVETTTPSKQSNK
								1	0.76	1.3	2.4	AAPSVTLFPPSSEELQANK

5.5 Lysine-specific demethylase 2B OS=Homo sapiens GN=KDM2B PE=1 SV=1

Protein Accession	sp Q8NHM5 KDM2B_HUMAN											
Mean Expression Ratio	1.31											
Median Expression Ratio	1.30											
Credible Interval	(0.685, 2.53)	0.25	0.5	1	2	4	A	2.5	50	97.5	Sequence	
Associated Peptides	1							1	0.76	1.5	2.9	QSDIFLGD
Associated Spectra	1											
Coverage	NaN											

5.6 Ig alpha-1 chain C region OS=Homo sapiens GN=IGHA1 PE=1 SV=2

Protein Accession	sp P01876 IGHA1_HUMAN											
Mean Expression Ratio	0.788											
Median Expression Ratio	0.789											
Credible Interval	(0.45, 1.37)	0.25	0.5	1	2	4	A	2.5	50	97.5	Sequence	
Associated Peptides	2							1	0.43	0.8	1.5	SAVQGPPER
Associated Spectra	2											
Coverage	NaN											

5.7 Collagen alpha-1(XV) chain OS=Homo sapiens GN=COL15A1 PE=1 SV=2

Protein Accession	sp P39059 COFA1_HUMAN											
Mean Expression Ratio	1.26											
Median Expression Ratio	1.26											
Credible Interval	(0.664, 2.44)	0.25	0.5	1	2	4	A	2.5	50	97.5	Sequence	
Associated Peptides	1							1	0.73	1.4	2.7	GATETASQ
Associated Spectra	1											
Coverage	NaN											

5.8 Ig mu chain C region OS=Homo sapiens GN=IGHM PE=1 SV=3

Protein Accession	sp P01871 IGHM_HUMAN											
Mean Expression Ratio	0.803											
Median Expression Ratio	0.804											
Credible Interval	(0.565, 1.14)	0.25	0.5	1	2	4	A	2.5	50	97.5	Sequence	
Associated Peptides	6							5	0.52	0.75	1.1	NVPLPVIAELPPK
Associated Spectra	17											
Coverage	NaN											

5.9 Fibrinogen beta chain OS=Homo sapiens GN=FGB PE=1 SV=2

Protein Accession	sp P02675 FIBB_HUMAN										
Mean Expression Ratio	1.23	0.25	0.5	1	2	4	A	2.5	50	97.5	Sequence
Median Expression Ratio	1.23						1	0.74	1.3	2.3	EEAPSLRPAPPISGGGYR
Credible Interval	(0.852, 1.79)						1	0.82	1.4	2.5	GGETSEMYLIQPDSSVKPYR
Associated Peptides	8						1	0.86	1.5	2.6	KGETSEMYLIQPDSSVKPYR
Associated Spectra	8						1	0.6	1.1	1.8	QGFQNVATNTDGK
Coverage	NaN						1	0.6	1.1	1.9	EDGGGWYNR
							1	0.69	1.2	2.1	QDGSVDFGR
							1	0.82	1.4	2.5	AAATQK
							1	0.64	1.1	1.9	DNENVVNEYSSELEK

5.10 Fibronectin OS=Homo sapiens GN=FN1 PE=1 SV=3

Protein Accession	sp P02751 FN1_HUMAN										
Mean Expression Ratio	1.23	0.25	0.5	1	2	4	A	2.5	50	97.5	Sequence
Median Expression Ratio	1.22						1	0.73	1.4	2.6	GNQESPK
Credible Interval	(0.707, 2.17)						1	0.66	1.2	2.3	TKTETITGFQVDAVPANGQTPIQR
Associated Peptides	2										
Associated Spectra	2										
Coverage	NaN										

5.11 Ig mu heavy chain disease protein OS=Homo sapiens PE=1 SV=1

Protein Accession	sp P04220 MUCB_HUMAN										
Mean Expression Ratio	0.833	0.25	0.5	1	2	4	A	2.5	50	97.5	Sequence
Median Expression Ratio	0.832						1	0.49	0.88	1.6	QVSGVTTDEVEAEAK
Credible Interval	(0.507, 1.37)						4	0.47	0.72	1.1	QDGEAVK
Associated Peptides	2										
Associated Spectra	5										
Coverage	NaN										

5.12 C4b-binding protein alpha chain OS=Homo sapiens GN=C4BPA PE=1 SV=2

Protein Accession	sp P04003 C4BPA_HUMAN										
Mean Expression Ratio	1.19	0.25	0.5	1	2	4	A	2.5	50	97.5	Sequence
Median Expression Ratio	1.18						1	0.65	1.2	2.3	LSLEIEQLELQFR
Credible Interval	(0.684, 2.08)						1	0.69	1.3	2.4	TWYPEVPK
Associated Peptides	2										
Associated Spectra	2										
Coverage	NaN										

5.13 Ig kappa chain C region OS=Homo sapiens GN=IGKC PE=1 SV=1

Protein Accession	sp P01834 IGKC_HUMAN										
Mean Expression Ratio	0.845	0.25	0.5	1	2	4					
Median Expression Ratio	0.847										
Credible Interval	(0.586, 1.21)						A	2.5	50	97.5	Sequence
Associated Peptides	6						3	0.61	0.94	1.4	IFPPSDEQLK
Associated Spectra	14						2	0.52	0.85	1.4	LLNNFYPR
Coverage	NaN						1	0.52	0.9	1.6	SQESVTEQDSK
							1	0.41	0.72	1.2	TVAAPSVFIFPPSDEQLK
							1	0.5	0.87	1.5	SVVCLLNNFYPR
							6	0.5	0.73	1.1	VDNALQSGNSQESVTEQDSK

5.14 Ig heavy chain V-III region VH26 OS=Homo sapiens PE=1 SV=1

Protein Accession	sp P01764 HV303_HUMAN										
Mean Expression Ratio	0.851	0.25	0.5	1	2	4					
Median Expression Ratio	0.854										
Credible Interval	(0.437, 1.65)						A	2.5	50	97.5	Sequence
Associated Peptides	1						1	0.41	0.8	1.6	EVQLLESGGGLVQPGGSLR
Associated Spectra	1										
Coverage	NaN										

5.15 Deducator of cytokinesis protein 1 OS=Homo sapiens GN=DOCK1 PE=1 SV=2

Protein Accession	sp Q14185 DOCK1_HUMAN										
Mean Expression Ratio	0.853	0.25	0.5	1	2	4					
Median Expression Ratio	0.856										
Credible Interval	(0.437, 1.61)						A	2.5	50	97.5	Sequence
Associated Peptides	1						1	0.40	0.79	1.6	GSCTISK
Associated Spectra	1										
Coverage	NaN										

5.16 EF-hand calcium-binding domain-containing protein 2 OS=Homo sapiens GN=EFCAB2 PE=2 SV=1

Protein Accession	sp Q5VUJ9 EFCB2_HUMAN										
Mean Expression Ratio	0.86	0.25	0.5	1	2	4					
Median Expression Ratio	0.864										
Credible Interval	(0.447, 1.66)						A	2.5	50	97.5	Sequence
Associated Peptides	1						1	0.41	0.81	1.6	FLPVMTEILLER
Associated Spectra	1										
Coverage	NaN										

5.17 Serum albumin OS=Homo sapiens GN=ALB PE=1 SV=2

Protein Accession	sp P02768 ALBU_HUMAN										
Mean Expression Ratio	1.16										
Median Expression Ratio	1.16	0.25	0.5	1	2	4	A	2.5	50	97.5	Sequence
Credible Interval	(0.753, 1.78)						1	0.66	1.2	2.1	AEFAEVSK
Associated Peptides	5						1	0.66	1.2	2.1	AVMDDFAAFVEK
Associated Spectra	5						1	0.63	1.1	2	LDELRDEGK
Coverage	NaN						1	0.7	1.2	2.2	LVAASQAALGL
							1	0.66	1.2	2.0	LVNEVTEFAK

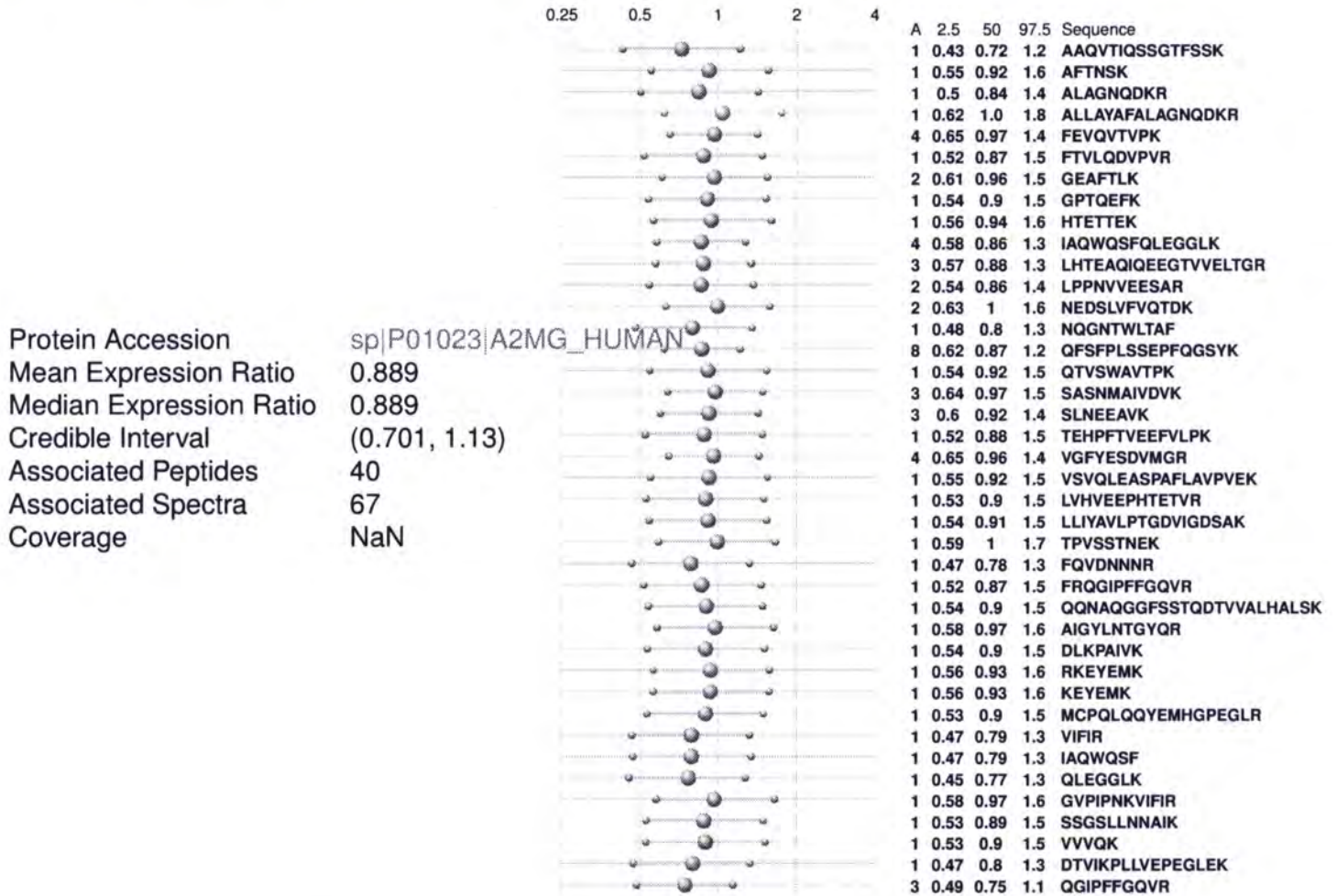
5.18 Ig heavy chain V-III region TEI OS=Homo sapiens PE=1 SV=1

Protein Accession	sp P01777 HV316_HUMAN										
Mean Expression Ratio	0.867										
Median Expression Ratio	0.869										
Credible Interval	(0.51, 1.47)	0.25	0.5	1	2	4	A	2.5	50	97.5	Sequence
Associated Peptides	1						6	0.55	0.8	1.2	EVQLVESGGGLVQPGGSLR
Associated Spectra	6										
Coverage	NaN										

5.19 Fibrinogen alpha chain OS=Homo sapiens GN=FGA PE=1 SV=2

Protein Accession	sp P02671 FIBA_HUMAN										
Mean Expression Ratio	1.14										
Median Expression Ratio	1.14	0.25	0.5	1	2	4	A	2.5	50	97.5	Sequence
Credible Interval	(0.83, 1.55)						2	0.83	1.3	2.1	ADSGEGDFLAEGGGVR
Associated Peptides	12						1	0.65	1.1	1.9	DSHSLTTNIMEILR
Associated Spectra	17						1	0.65	1.1	1.9	DYEDQQK
Coverage	NaN						2	0.82	1.3	2.1	GGSTSYGTGSETESPR
							3	0.8	1.2	1.9	GLIDEVNQDFTNR
							1	0.62	1.1	1.8	GSESGIFTNTK
							1	0.54	0.94	1.6	NPSSAGSWNSGSSGPGSTGNR
							1	0.68	1.2	2	NSLFEYQK
							1	0.66	1.1	1.9	QLEQVIK
							2	0.75	1.2	1.9	TFPGFFSPMLGEFVSETESR
							1	0.63	1.1	1.8	QHLPLIK
							1	0.63	1.1	1.9	EVDLKDYEDQQK

5.20 Alpha-2-macroglobulin OS=Homo sapiens GN=A2M PE=1 SV=1



5.21 Fibrinogen gamma chain OS=Homo sapiens GN=FGG PE=1 SV=3



5.22 Complement C4-B OS=Homo sapiens GN=C4B PE=1 SV=1; Complement C4-A OS=Homo sapiens GN=C4A PE=1 SV=1

Protein Accession	sp P0C0L5 CO4B_HUMAN sp P0C0L4 CO4A_HUMAN	
Mean Expression Ratio	1.10	
Median Expression Ratio	1.09	
Credible Interval	(0.575, 2.09)	0.25 0.5 1 2 4 A 2.5 50 97.5 Sequence
Associated Peptides	1	1 0.6 1.1 2.2 ALEILQEEDLIDEDDIPVR
Associated Spectra	1	
Coverage	NaN	

5.23 Abnormal spindle-like microcephaly-associated protein OS=Homo sapiens GN=ASPM PE=1 SV=2

Protein Accession	sp Q8IZT6 ASPM_HUMAN	
Mean Expression Ratio	1.06	
Median Expression Ratio	1.06	
Credible Interval	(0.546, 2.06)	0.25 0.5 1 2 4 A 2.5 50 97.5 Sequence
Associated Peptides	1	1 0.55 1.1 2.1 LQIRSSV
Associated Spectra	1	
Coverage	NaN	

5.24 Complement C3 OS=Homo sapiens GN=C3 PE=1 SV=2

Protein Accession	sp P01024 C3_HUMAN	
Mean Expression Ratio	1.05	
Median Expression Ratio	1.05	
Credible Interval	(0.717, 1.53)	0.25 0.5 1 2 4 A 2.5 50 97.5 Sequence
Associated Peptides	8	1 0.49 0.87 1.5 EDIPPADLSDQVPDTESETR
Associated Spectra	8	1 0.59 1.0 1.8 EGVQKEDIPPADLSDQVPDTESETR
Coverage	NaN	1 0.6 1.0 1.8 ILLQGTPVAQMTEDAVER
		1 0.71 1.3 2.2 SGSDEVQVGQQR
		1 0.56 1 1.7 TSSSGQQTQQR
		1 0.55 0.96 1.7 DDFVPPVVR
		1 0.64 1.1 2.0 SNLDEDIAEENIVSR
		1 0.68 1.2 2.0 KQELSEAEQATR

5.25 von Willebrand factor OS=Homo sapiens GN=VWF PE=1 SV=2

Protein Accession	sp P04275 VWF_HUMAN	
Mean Expression Ratio	0.958	
Median Expression Ratio	0.96	
Credible Interval	(0.54, 1.67)	0.25 0.5 1 2 4 A 2.5 50 97.5 Sequence
Associated Peptides	2	1 0.55 1.0 1.9 AVVILVTDVSVDSVDAADAAR
Associated Spectra	2	1 0.47 0.89 1.6 VKEEVFIQQR
Coverage	NaN	

5.26 Ferritin light chain OS=Homo sapiens GN=FTL PE=1 SV=2

Protein Accession	sp P02792 FRIL_HUMAN						
Mean Expression Ratio	0.957						
Median Expression Ratio	0.963						
Credible Interval	(0.544, 1.68)	0.25	0.5	1	2	4	A 2.5 50 97.5 Sequence
Associated Peptides	1						3 0.59 0.93 1.5 LGGPEAGLGEYLFER
Associated Spectra	3						
Coverage	NaN						

5.27 DENN domain-containing protein 4B OS=Homo sapiens GN=DENND4B PE=1 SV=4

Protein Accession	sp O75064 DEN4B_HUMAN						
Mean Expression Ratio	1.03						
Median Expression Ratio	1.03						
Credible Interval	(0.567, 1.89)	0.25	0.5	1	2	4	A 2.5 50 97.5 Sequence
Associated Peptides	1						2 0.6 1.0 1.8 AGGRQDEAGTPRR
Associated Spectra	2						
Coverage	NaN						

5.28 Transmembrane protease, serine 13 OS=Homo sapiens GN=TMPRSS13 PE=2 SV=2

Protein Accession	sp Q9BYE2 TMPSD_HUMAN						
Mean Expression Ratio	1.02						
Median Expression Ratio	1.02						
Credible Interval	(0.533, 1.97)	0.25	0.5	1	2	4	A 2.5 50 97.5 Sequence
Associated Peptides	1						1 0.53 1.0 2.0 NKPGVYTK
Associated Spectra	1						
Coverage	NaN						

5.29 Histidine-rich glycoprotein OS=Homo sapiens GN=HRG PE=1 SV=1

Protein Accession	sp P04196 HRG_HUMAN						
Mean Expression Ratio	1.00						
Median Expression Ratio	1.00						
Credible Interval	(0.521, 1.93)	0.25	0.5	1	2	4	A 2.5 50 97.5 Sequence
Associated Peptides	1						1 0.52 1 2.0 DHHHPHKPHEHGPPPPDER
Associated Spectra	1						
Coverage	NaN						

5.30 Sulfate transporter OS=Homo sapiens GN=SLC26A2 PE=1 SV=2

Protein Accession	sp P50443 S26A2_HUMAN										
Mean Expression Ratio	1										
Median Expression Ratio	1										
Credible Interval	(0.52, 1.91)	0.25	0.5	1	2	4	A	2.5	50	97.5	Sequence
Associated Peptides	1						1	0.52	0.99	2.0	MSEESK
Associated Spectra	1										
Coverage	NaN										